University of Groningen

Bachelor Thesis

The Habitability of Exoplanets

Author:
Marrick Braam
S2775298

Supervisor:
prof. dr. F.F.S. van der Tak

A thesis submitted in fulfillment of the requirements for the degree BSc in Astronomy

Faculty of Science and Engineering
Kapteyn Astronomical Institute

July 6, 2017

Abstract

In recent years the number of known exoplanets has exploded to around 3500, but the majority of these planets are inhospitable to life as we know it. This thesis presents research on the habitability of exoplanets, by first reviewing the different criteria that define a habitable environment and after that computations of some parameters for habitability. Different solvents have been considered in computing the parameters, namely H_2O, CH_4, NH_3 and N_2. Planetary albedo has a strong influence on the planetary equilibrium temperature, therefore it is an important factor in defining the habitability. Another important constraint is the solid surface limit, which excludes gas and ice giants. The maximum eccentricity to keep a planet inside the Habitable Zone(HZ) during its orbit ranges from 0.746 up to 0.844 for different solvents. This is satisfied by 98 to 99% of planets with known eccentricity. Even though the maximum eccentricity is dependent on where in the HZ the planet is located, it has a small impact in constraining the number of habitable planets. Applying the parameters leads to nine planets from the NASA Exoplanet Archive that might be considered candidates to be habitable, according to the criteria discussed here. This is out of 600 planets left, the others have one or more of the important parameters missing in the archive. Furthermore it has been found that the amount of atmospheric CO_2 strongly influences the equilibrium temperature and therefore the outer limit of the Habitable Zone. For already the near future, the search for exoplanets will be focused on Earth-like planets and somewhat larger rocky planets. In addition atmospheric compositions will be studied using transit spectroscopy and hence a habitable exoplanet might be confirmed.

Contents

1 Introduction

Up to the 15th of May 2017 a total number of 3486 exoplanets have been discovered and confirmed[1]. In Figure 1 the cumulative amount of discoveries is shown per year, from the first discovery made in 1989. The figure also shows the method with which the exoplanets have been discovered. It can be seen that the first exoplanet has been discovered in the year 1989, but especially in the last ± 5 years the amount of discovered exoplanets has exploded. For the coming years this amount is expected to experience an even larger growth. The question is whether or not some of these planets are capable of supporting the existence of life, either life as we know it or maybe even completely unexpected forms of life. As a step toward this goal, this thesis presents research into what criteria are to be fulfilled in order for life being able to form. The search for extraterrestrial life is already going on since the beginning of civilization, but is getting more and more attention since around halfway the twentieth century[2]. As Sara Seager stated beautifully: "Humanity will always have a strong desire to search for a place like home." (Seager and Deming, 2010)

This thesis will start with some introductory information, including detection methods and the definition of habitability classes in Section 1. In Section 2 the most important criteria for habitability will be discussed, both astrophysical and geophysical. The concept of the planetary equilibrium temperature will be discussed in Section 3, with the emphasis on the influence of the planetary Bond albedo. This discussion is extended to the definition of the Habitable Zone, including the influence of greenhouse gases (in particular CO_2) in Section 4. Section 5 discusses the influence of one of the extraterrestrial climatological variables: the eccentricity of planetary orbits. Then a discussion is done about whether the state of a planetary surface is relevant in Section 6. The various discussed criteria are put together in the discussion done in Section 7, leading to an estimate of the number of planets capable of the support of life. Hence this leads to the conclusion, which can be found in Section 8. After that, an outlook for discoveries in the nearby future will be given.

[1] from the NASA Exoplanet archive: https://exoplanetarchive.ipac.caltech.edu/index.html

[2] History of the Search for Extraterrestrial Life (SETI): https://history.nasa.gov/seti.html

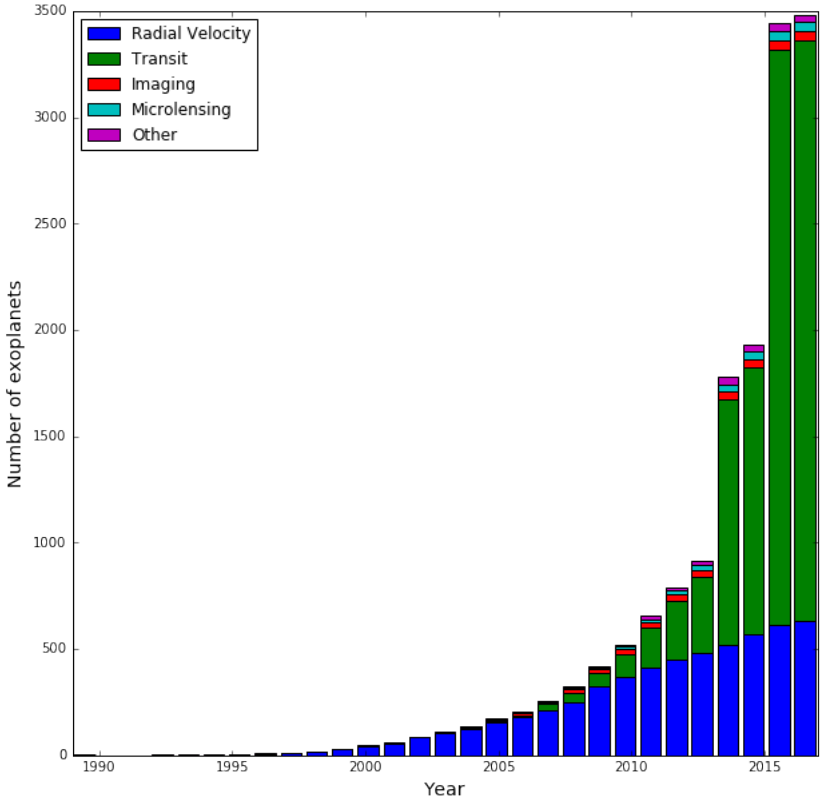

Figure 1: The cumulative number of exoplanets found per year. Also the methods with which the exoplanets are found are colour-coded in their associated number of discoveries[1].

1.1 Detection methods

The four most important exoplanet detection methods are transit photometry, radial velocity, high contrast imaging and microlensing (Robinson, 2017). Although there are other detection methods, the discussion here will be limited to these four since the other methods have such a small impact on the number of detections, as can be seen in Figure 1.

Transit photometry takes a measure of the fractional dimming of stellar brightness due to a planet transiting its host star. Even though the probability of a transit being on the line-of-sight to a star is low, the transit method is in particular very efficient by observing large amount of stars (10^4) simultaneously, delivering the biggest amounts of exoplanets known so far. The transit method is used to get measurements of the size of planets, leading to the discovery of large numbers of planets in the range $R_\oplus < R_P < 4R_\oplus$ (Fischer et al., 2015), which happens to be unpopulated for planets in our Solar System. Besides that this method can be used to determine a planet's orbital period(Fischer et al., 2015). On top of that, by using transit spectroscopy one can detect features of a planetary atmosphere by carefully studying the spectral lines (Seager and Deming, 2010).

The radial velocity method is based on the gravitational pull from a planet on its host star, resulting in a displacement of the parent star's radial velocity and hence a Doppler shift in the spectral lines sent out by the star. Hence it is most conveniently used to detect either high mass planets or planets in a close orbit, since both situations have a detectable gravitational force involved (Fischer et al., 2015). The radial velocity method leads to measurements of a planet's orbital period, eccentricity and semi-major axis and a lower limit of the mass.

In high contrast (or direct) imaging the faint point spread functions of planets are resolved from their host star PSF by using optical techniques, for example coronagraphy or interferometry. One would then need to measure the planet-to-star flux ratio $\frac{F_P}{F_*}$ (Robinson, 2017). This is mostly applicable to planets in a wide orbit around their host star, with the ability to reflect light of their host star and thereby becoming self-luminous. This method gives measurements of the planets effective temperature and may tell something about planetary

mass. In addition, by studying the planet's spectra one might find information about the atmospheric composition of the planet. Although not used that much yet due to the problem of blocking out the adjacent host star, this method might lead to a lot of new discoveries since it is especially capable of finding planets at large orbits, contrary to the transit or radial velocity method (Seager and Deming, 2010).
Microlensing occurs when a star, that is aligned with another star, bends the light of the latter gravitationally. Planets that are gravitationally bound to the lens star lead to perturbations in the light curve seen from the source star. This technique may lead to measurements of the planetary mass and the distance to the host star (Fischer et al., 2015).
Generally the different techniques are complementary to each other. For example, since transit photometry can also lead to false measurements of an exoplanet by having a brightness dip due to stellar variability or an eclipsing binary star, the radial velocity method can be used to confirm or decline the detection. This combination may then lead to a measurement of the true mass of the planet(Fischer et al., 2015).

1.2 Habitability Classes

Habitability gives a measure of the potential of a planet or an associated satellite to have environments that are able to develop and sustain life. They do not necessarily need to contain life. Habitable planets can be sorted into four different classes (Lammer et al., 2009). Class I planets are Earth-like planets on which the astro- and geophysical conditions are such that complex life forms as we know it may evolve on the surface. Class II contains the planets on which the initial conditions were sufficient to support the evolution of life, but on which the astro- and geophysical conditions resulted in different environmental conditions such that life evolved in a different way compared to Earth or did not develop at all. Hence they are located inside the Habitable Zone of their host star, but are unable to support life in the way as we know it. Examples of Class II planets are Venus, on which the high density of greenhouse gases caused a temperature rise that resulted in a very dry environment or the cold Martian environment, which lost large parts of its atmosphere due to the absence of a strong intrinsic magnetic field (Jakosky et al., 2015)(Kass and Yung, 1995). Class III planets have an inventory of subsurface H_2O available. An example of this is Europa, one of the moons of Jupiter. On Europa, the H_2O inventory is even in contact with silicates, which could play the role of nutrients in the biochemistry (Lammer et al., 2009). Finally, Class IV are environments that have two layers of ice both above and below a layer of liquid H_2O (examples include the moons Enceladus, Ganymede and Callisto) and/or liquids above ice (for example Titan).

2 Criteria for Habitability

Several criteria are involved to asses a qualitative description of exoplanet habitability. These include both astrophysical and geophysical criteria. This section reviews some of the most important criteria. Not all criteria are applicable to the data in the Archive. Therefore Subsection 2.8 contains a discussion about which criteria are considered in this thesis.

2.1 Availability of a solvent

Every form of life as we know it is dependent on liquid water to be able to metabolize and reproduce (Güdel et al., 2014), even life that is able to survive for a very long time without H_2O. Other important functions of liquid H_2O as the solvent in which life emerges and evolves include its capability to form Hydrogen bonds and stabilization of macromolecules (Lammer et al., 2009). For example the Hydrogen bonds increase the boiling point of H_2O and result in a dipole moment for H_2O, which helps in dissolving other molecules that are also slightly charged.
An important concept in defining habitability is the Habitable Zone(HZ), which is the zone around a star in which planets are able to support the presence of liquid H_2O, given sufficient pressure conditions. However, this is the case for terrestrial life, which is mostly Carbon-based (Pace, 2001). The possibility of life based on a different biochemistry can not be excluded. The only difference discussed in this thesis is the possibility of another solvent instead of H_2O. A nearby example of this is the possibility of life on Saturn's moon Titan, where liquid methane (CH_4) is so common that it might perform the role of the solvent (McKay and Smith, 2005). The Cassini-Huygens spacecraft detected lakes of CH_4 on Titan in 2005. Other solvents that have been discussed include ammonia (NH_3) and nitrogen (N_2)(Schulze-Makuch and Irwin, 2006). In the discussion about other solvents in this thesis, the definition of the HZ will be extended to the different liquid ranges of the various solvents. The

ability of a planet to maintain its inventory of solvent is dependent on the surface temperature, for H_2O this temperature should range between the freezing point of H_2O and the boiling point of H_2O (Ribas et al., 2016)(Seager, 2013). Since these transition points are however dependent on the pressure, the points used are based on the standard pressure of 1.013bar. Using a biochemistry based on another solvent will also adjust the temperature range. This can be seen in Table 1. The planetary surface pressure is provided by an atmosphere, for example the thin Martian atmosphere provides a pressure of only $6 - 9$ mbar, while Earth's atmosphere results in a pressure of 1.01325 bar. Increasing the pressure will increase the boiling point of H_2O, while the freezing point will roughly stay the same. Hence the radial extent of the HZ will increase (Vladilo et al., 2013). To define a minimum atmospheric pressure for a specific solvent-based planet one would have to look at the phase diagram of the solvent to see for what pressures it could still be in the liquid phase. These pressures are the triple points shown in Table 1.

Solvent	Freezing Point [K]	Boiling Point [K]	Triple Point [bar]
H_2O	273.15	373.12	6.11×10^{-3}
CH_4	90.69	111.67	1.17×10^{-1}
NH_3	195.41	239.82	6.11×10^{-2}
N_2	63.15	77.35	1.24×10^{-1}

Table 1: The freezing and boiling points of some possible solvents on which life could be based [3], for the standard pressure of 1.013 bar. Also the triple points and the associated minimum pressures are shown.

2.2 Initial inventory of volatiles

Even though a planet may have the right circumstances to be able to maintain its inventory of liquid H_2O, it is still needed to at least have an initial inventory of H_2O. To be able to comprehend this, one will have to look at the formation of the planets. For Earth the idea is that impacts of H_2O rich bodies played a crucial role in delivering its H_2O inventory (Morbidelli et al., 2000). Most of these impacts happened with asteroids, of which the drier and stonier S-types are mostly located at smaller radii than the inner radius of the asteroid belt at 2.7 AU and the more H_2O- and volatile-rich C-group asteroids are located at larger radii (DeMeo and Carry, 2013). Hence collisions with the latter are thought to be essential in the Earth attaining its initial H_2O inventory, both in the classical accretion model and the Grand Tack model(O'Brien et al., 2014) (Raymond and Morbidelli, 2004). This H_2O delivery can however be very different for other planets, since it is dependent on the formation history of planets in the specific stellar system. Another possibility for the initial H_2O inventory of a planet may be the formation of the planet in the outer parts of the stellar system, and migration inwards at later times (Paardekooper et al., 2011). This way, its initial H_2O content would also have been affected. Other mechanisms affecting the planet's H_2O inventory can be external photoevaporation or bombardments of H_2O-rich bodies in late times (Ribas et al., 2016).

H_2O belongs to a larger group of chemical substances that are necessary for a planet to be habitable, known as volatiles. The compounds formed by elements as C, O, H, N, P and S are called volatiles since they are typically gases or liquids at room temperature (Güdel et al., 2014). Therefore, the group of volatiles includes H_2O. The amount of volatiles is also expected to have originated from collisions with bodies found in the asteroid belt or beyond it (Raymond and Morbidelli, 2004). Next to that a part of the volatile inventory will be around on the planet after its formation. The required environmental conditions and the amount of time in which the important volatiles stay intact should be sufficient in order for life to form (Lammer et al., 2009). A planetary atmosphere is needed in order to prevent loss of the volatile inventory.

2.3 Role of atmosphere

An atmosphere protects the volatile inventory from escaping into outer space, but also prevents important molecules made of volatiles from being destroyed via absorption of stellar radiation (Ribas et al., 2016): the atmosphere protects the surface from XUV radiation (which includes far and extreme ultraviolet and X-rays), especially via its ozone layer. In addition it offers protection against incoming solar winds and cosmic rays,

[3]From Gas Encyclopedia Air Liquide: https://encyclopedia.airliquide.com

which will collide with atmospheric particles. Another protection atmospheres supply is preventing a lot of meteor impacts.
The atmospheric composition and density defines the climate on terrestrial planets, it provides wind and a weather cycle, a pressure that is needed to have a solvent in liquid form and a temperature rise particularly via the presence of greenhouse gases (Turbet et al., 2016). Examples of greenhouse gases are H_2O, CO_2, O_3, CH_4 and N_2O (Güdel et al., 2014). These gases have the ability to absorb infrared radiation coming in from the host star and re-emitting it, so that the lower atmosphere is heated. An extreme example of this greenhouse effect is seen on Venus, where the large amount of CO_2 is responsible for the strong absorption of IR radiation and hence for the high temperature of 737K. On Earth the greenhouse effect leads only to a temperature of 306.15K (Güdel et al., 2014). The situation on Venus is knows as a runaway greenhouse effect: the interplay between planetary surface temperature and the density of greenhouse gases in the atmosphere gives rise to a great increase in temperature, which will result in complete evaporations of oceans (Kopparapu et al., 2016).
A planet's albedo also has to be taken into consideration, which indicates the fraction of radiation that is reflected from the planet (Kopparapu et al., 2016). This is partly due to atmospheric reflection, although also the surface contributes to the reflection of radiation. The albedo effect can greatly influence the planetary temperatures. For example, a planet with a thick cloud deck reflects a lot of stellar flux, causing the planet to cool down. Without this albedo, the stellar flux would cause a larger temperature rise.

2.4 Stellar Activity

The host star itself is also an important factor in defining the habitability of exoplanets. Its most important function is to deliver heat and hence energy to planets. All life will need a certain form of energy in order to emerge and substain. Even though as far as we know life only emerged around a G-type star, the search for habitable exoplanets should be extended to K, M and F-type stars. The hotter O, B and A stars do not have to be taken into consideration, since they are too luminous and have relatively short lifetimes, so that it can be considered impossible for life to form in these systems. This can be justified by comparing the stellar lifetime to the time it took life to form here on Earth. The Earth is $(4.55 \pm 0.01) \times 10^9$ years old (Manhes et al., 1980). It took 300 to 800 million years for the first life forms to develop (Dodd et al., 2017), while the first signs of multicellular life date back to around 3×10^9 years. The stellar lifetimes of O, B and A stars range from 2×10^6 to 1.9×10^9 years [4], therefore planets around them might only be able to develop single-celled lifeforms. F-type stars should be included in discussing the possibility of the system harboring life, since their lifetime ranges from 1.6 to 6.9 billion years[4].
Since the host star has activity in many bands of the electromagnetic spectrum, its output can also be destructive for the emergence of life. Therefore part of this activity has to be blocked by an atmosphere, in order to have an environment that is habitable. Energy production in stellar cores via the nuclear fusion is responsible for a star's photospheric output (Güdel et al., 2014). This process hence determines the effective temperature and the luminosity. Planetary atmospheres are then influenced by stars via XUV-rays, flares, stellar winds and Coronal Mass Ejections (CME's) (Kaltenegger and Traub, 2009). They originate from a release of magnetic energy in the star, and are hostile to the emergence of life due to their biological impact. Next to that, flares, stellar winds and CME's can result in the erosion of planetary atmospheres (non-thermal escape). Therefore a planet would need protection against it in the form of a magnetic field, which deflects charged particles.
In addition, the output stellar flux has a big influence on the planetary temperature and hence mostly defines the edges of the Habitable Zone, which is discussed in Section 4). The smaller the stellar luminosity, the smaller the distance between the star and the HZ (Seager and Deming, 2010).
All stars experience changes in their luminosity, which may be fatal to the evolution of life if these fluctuations are so extreme that life cannot adapt to the fast temperature and radiation level variations. Hence a star should be relatively stable in time. Figure 2 is a plot of stellar activity versus the rotation rate over the convective turnover time. The convective turnover time is the time it takes for convection to completely replace the matter in a certain region.

[4]Lifetime values taken from http://www.atlasoftheuniverse.com/startype.html

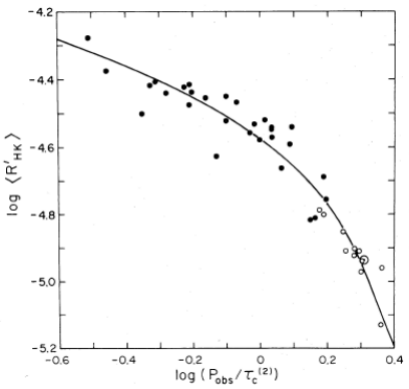

Figure 2: A plot of stellar activity indicator R'_{HK} versus the rotation period over the convective turnover time. Closed dots indicate young stars and open stars indicate old (late-type) stars. From Noyes et al., 1984 (Noyes et al., 1984).

From this figure it can already be seen that the stellar activity is lower for late-type stars, which are the open dots. This means that late-type stars are the more stable stars and hence it can be concluded again that they are the favorable stellar candidates for the emergence of life around them. Thus the search for habitable planets should be limited to stars with a spectral type of M, K and G, while F-type stars might also still be able to supply the right stellar conditions.

2.5 Climate Cycles

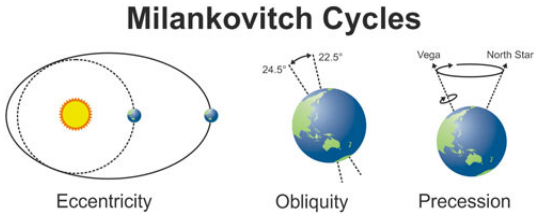

Figure 3: Illustration of the concepts of eccentricity, obliquity and precession.

The climate on Earth varies with time depending on the so-called Milankovitch Cycles. These Cycles include the eccentricity of the planet's orbit, the obliquity and the precession. The three parameters also apply to exoplanets.
The eccentricity measures how far from circularity the orbit of the planet is, and hence leads to a change in the distance to its host star as the planet revolves one orbit. An orbit with a high eccentricity might lead to strong climate changes, for example the Earth may turn into a snowball when it is located around the apoastron of the elliptical orbit. This is thought to be one of the main reasons of the ice ages that have been experienced on Earth in the past (Spiegel et al., 2010). A variation in Earth's eccentricity would lead to stronger or smaller differences in different seasons, since the difference between the semi-major and semi-minor axis will increase or decrease respectively. Both a high eccentricity and strong variations in eccentricity are hostile to the emergence of life. Therefore new criteria can be deduced that has to be satisfied by the planet: the eccentricity of a planet must be small enough to prevent the planet's orbit from exceeding the boundaries of the Habitable Zone and a planet's orbit should be relatively constant. The first of these criteria will be discussed in Section 5, while the other can not yet be measured for exoplanets and hence is left out of the discussion.
The obliquity is defined as the axial tilt of a planet, and hence leads to seasonal variations on a planet. Increasing the obliquity would lead to increased stellar flux at locations with a higher altitude and decreased stellar flux at lower altitudes, hence lowering the latitudinal temperature gradient (Spiegel et al., 2010). Since the increase in flux received by the poles exceeds the decrease experienced at the equator, this will lead to a global rise of temperature.
Precession comes in two different ways, namely axial and periastron precession. Axial precession is related to the obliquity of a planet, the axial tilt is responsible for a movement of the rotational axis in time: it will trace out a cone (displayed in Figure 3). Periastron precession is the rotation of the planetary orbit around the host star. An example of this is the orbit of Mercury around the sun (Clemence, 1947). Both of these precessions lead to a slow change in the position of solstices and equinoxes relative to the periastron and apoastron, and hence adjust the lengths of seasons.
For exoplanets however, the obliquity or precession can not be measured, and hence these will be left out in the discussion on their influence on habitability. Eccentricity has been measured for 1068 of the now known exoplanets, and hence is worth some discussion.

2.6 Geological criteria

Essential geological conditions include the presence of a solid or perhaps liquid surface. For exoplanets this is however not as easy to find out as for Solar System planets. There are robust theories that predict that planets with a mass exceed-

ing $10M_{\oplus}$ will attract lots of gas from the stellar nebula and become gas or ice giants (Mizuno et al., 1978). Similarly, as far as we know planets that have a radius $> 2R_{\oplus}$ are gas or ice giants(Weiss and Marcy, 2014). On the other side a planet's mass should also be sufficiently large for three reasons. Firstly the planet needs to be able to generate gravity that is strong enough to be able to preserve its atmosphere. Secondly a planet with a mass that is too small will not be able to generate geological activity and hence will lose the energy from its formation, ending up geologically dead. The final reason is that a planet with a mass that is too low will not be able to produce a magnetic field. This lower mass limit is roughly calculated to be $0.3M_{\oplus}$ (Ikoma and Genda, 2006). Applying this lower limit to the Solar System planets would lead to contradictions: Mars and Mercury are two planets that have a mass smaller than $0.3M_{\oplus}$. Even though Mercury indeed lacks an atmosphere, it still has a magnetic field around it and shows signs of geological activity. Mars is indeed missing a magnetic field, but still shows geological activity. Next to that, the pressure of Mars' atmosphere is above the pressure of the triple point, and therefore this calculated limit will not be used in the discussion done here.

Another geological criteria is plate tectonics and thus mantle convection. Without it the Carbon-cycle on Earth would not have existed and a planet would get trouble stabilizing the surface temperature(Kasting and Catling, 2003). The absence of plate tectonics could be one of the reasons for the extremely high temperatures on Venus.

2.7 Other criteria

Furthermore, planetary rotation is a factor in the determination of habitability (Kopparapu et al., 2016). A slowly rotating planet has a smaller difference in temperature between the poles and the equator compared to a planet rotating at a high rate. This might result in the buildup of clouds at the substellar point, which are optically thick and hence have a strong impact on the planetary albedo. Hence this leads to blocking more of the incoming stellar light, stabilizing a planet that is too close to its host star against a runaway greenhouse (known as cloud stabilization) (Kopparapu et al., 2016). The opposite is true when a planet rotates faster: the boundaries of the HZ will be farther away from the host star due to stronger temperature difference between equator and poles and hence a lower planetary albedo.

Planets that are close to their host star feel a strong gravitational force from it and can become tidally locked, hence facing their host star with one side for all the time. This then leads to synchronous rotation (Griessmeier et al., 2005). For M-type stars, it is known that the region in which tidal locking could occur overlaps with its HZ, leading to the possibility of habitable planets rotating synchronously around their host star (Griessmeier et al., 2005). The effect of this is obvious: one side could have temperatures around the boiling point while the other side may be well below the freezing point of H_2O. Hence on the day side this could lead to atmospheric escape, while the night side might experience atmospheric collapse: freezing of its constituents (Hu and Yang, 2014). A tidally locked planet would need (a combination of) atmospheric and/or ocean heat transport in order to get habitable environments on certain fractions of the planet (Yang et al., 2013)(Hu and Yang, 2014). These processes could lead to a temperature which is supportive for the existence of life.

The last criteria discussed is the existence of a planetary magnetic field in order to protect it from destructive radiation and atmospheric erosion (Güdel et al., 2014). This includes the deflection of charged particles from solar winds and cosmic rays. For the field to be protective, the base of the magnetosphere should always extend farther than the height of the outer layers of the exosphere. A planet will need an iron core and need to rotate fast enough in order to generate the magnetic dynamo that induces an intrinsic magnetic field. Another possibility would be the induction of an external magnetic field, which is the case for Venus (Luhmann and Cravens, 1991). This magnetosphere is generated by the interaction between the ionosphere of Venus and solar wind particles, deflecting the latter.

2.8 Applicable criteria

Although many possible criteria for habitability exist, as can be seen from the previous sections, not all criteria are equally relevant in the research here. The ability of a planet to maintain the solvent available will be researched by looking at the equilibrium temperatures of planets, under the assumption of a standard pressure on the planet since the planet specific pressures are unknown at this moment. This will partly include the influence of atmospheres, by considering the Bond albedo and the effect of greenhouse gases (namely CO_2). Next to that the equilibrium temperature depends on stellar luminosity, however this will not include variations in stellar activity, since not

enough is known about it for most stars. Even though a planet may have a temperature range favorable for the existence of a solvent (and hence also volatiles), it may still lack the presence of volatiles. This can however only be found by spectroscopy of the exoplanets, and for many of them this has not yet been done. As discussed before, the Milankovitch cycles will only be studied by the eccentricity of exoplanet orbits. Again the reason for this is a lack of knowledge about obliquity and precession of exoplanets. The geological criteria, including geological activity and the presence of a magnetic field are left out in the research here, since much more research should be done on the exoplanets themselves to know whether or not they contain this. Tidal locking will be discussed by considering the so-called redistribution factor. The last criteria that can be checked is the presence of a solid or a liquid surface, at least excluding the attraction of great amounts of gas.

3 Equilibrium temperature and albedo influence

This section starts with a discussion of the concept of the equilibrium temperature, including its limitations. This concept is applied to exoplanets, at first for the single planet TRAPPIST-1c in Subsection 3.2 to see what the influence of the albedo is on the equilibrium temperature. Then the temperatures for the exoplanets with the known necessary quantities are calculated in Subsection 3.3. From this the number of habitable planets in the different solvent ranges are determined as a function of albedo.

3.1 Concept of Equilibrium Temperature

The equilibrium temperature of an exoplanet is the temperature it would have if it were a blackbody only receiving radiation from its host star. This temperature is frequently used as an approximation since we usually do not know the emissivity of the exoplanet (Seager, 2010). Therefore we assume an emissivity equal to unity, which is the case for a blackbody. Real objects have an emissivity lower than unity, which will result in a higher temperature for the planet.
The equilibrium temperature is found by balancing a planet's heating and cooling processes under assumptions that are highly idealized. The power that is absorbed by the planet is assumed to only consist of the heat output of the host star and is given by:

$$P_{\text{abs}} = S r_p^2 (1 - A) \qquad [\text{W}] \tag{1}$$

Where S is the stellar flux, r_p is the planetary radius and A is the Bond albedo, which ranges from 0 to 1. An albedo of 1 means that all radiation is reflected by the planet, while all radiation is absorbed if the albedo is equal to 0. For Earth, the albedo is made up of several different surfaces, which results in the albedo being 0.306. The cooling process is the energy re-radiated back into space by the planet, and can be described as an emitted power:

$$P_{\text{rad}} = 4\pi r_p^2 \sigma T^4 f \qquad [\text{W}] \tag{2}$$

Where σ is the Stefan-Boltzmann constant. The factor f is called the redistribution factor. If all incident energy is uniformly redistributed on the planetary sphere, $f = 4$. If the energy is uniformly distributed over the starlit hemisphere (thus the dayside of the planet), $f = 2$. Hence this factor includes the tidal locking of a planet: a planet with $f = 2$ can be seen as a planet facing its host star with the same side during its lifetime. By putting these two equations equal to each other we can solve for the effective temperature in K(Selsis et al., 2007):

$$T_{\text{eq}} = \left(\frac{S(1-A)}{f\sigma}\right)^{0.25} = \left(\frac{L_*(1-A)}{4\pi a^2 f\sigma}\right)^{0.25} \tag{3}$$

The stellar flux has been rewritten into luminosity, therefore we have the factor a representing the distance of the planet to the host star. Hence we can see that a planet's equilibrium temperature is dependent on the distance to its host star, but not on the planetary radius. Next to that the albedo effect and the redistribution of heat play a big role in the (both equilibrium as well as true surface) temperature of a planet.

3.2 Limitations of the equilibrium temperature

Equation 3, although useful to compute the temperature of radiating planets, has some conceptual limitations (Seager, 2010). First it neglects non-radiative heating and cooling mechanisms, for example it assumes the planet does not produce and thereby radiate its own heat from its core. This is not true for giant planets like Jupiter and neither for Earth, since it generates internal heat via plate tectonics and volcanism. Taking this self-luminosity into consideration would hence lead to a higher temperature. Secondly the equilibrium

temperature does not include atmospheric influence properly, initially it even assumes a naked planet (no atmosphere). However, changing the values of the albedo and/or the redistribution factor can represent some of the atmospheric influences, since the atmosphere is partly responsible for reflecting incoming radiation and redistribution of the incident energy over the planetary surface. Third, the true temperature of a planet depends on the properties of re-emission of energy, which is not taken into consideration. The gases in a planetary atmosphere each absorb and re-emit radiation of different wavelengths in a more efficient way. Finally, the equation is often used in calculating atmospheric temperatures. In doing so, one must keep in mind that atmospheres have a certain temperature profile. Hence, calculating the equilibrium temperature in order to say something about atmospheric or surface temperatures of planets with a dense atmosphere must be done with great caution: there is a possibility that the actual surface temperature differs significantly from the calculated equilibrium temperature. To show this we calculate the equilibrium temperatures for the Solar planets, as shown in Table 2. The last column contains the mean surface temperature as measured for the different planets. Hence the calculations of the equilibrium temperature lead to reasonable values for Mercury and Mars, since both of these have a negligible atmospheric influence. The difference with the mean surface temperature for Earth and Venus' temperature are explained by the influence of their greenhouse effect, as discussed in Subsection 2.3. This illustrates the fact that calculations of equilibrium temperature can contain significant systematic errors.

Planet	T_{eq} for f=2 [K]	T_{eq} for f=4 [K]	Mean surface temperature [K]
Mercury	522.76	439.59	440
Venus	269.53	226.65	737
Earth	302.11	254.04	288
Mars	249.56	209.86	210

Table 2: Equilibrium temperatures calculated for the inner four planets of the Solar System. The last column contains their mean surface temperature[5].

3.3 TRAPPIST-1 system: planet c and its equilibrium temperature

The planetary system around the star TRAPPIST-1 is a recently found system, with a total number of seven planets orbiting the host star (Gillon et al., 2017). The planets in the system are much closer to the star than the usual distances in the Solar System, at distances ranging from 0.111 AU to a maximum of 0.0451 AU. Since TRAPPIST-1 is an ultra cool M-dwarf (effective temperature of 2559K), the planets around it could still show signs of habitability. Planet c has been chosen here as a target to compute its equilibrium temperature, and hence to see whether this temperature allows the existence of liquid H_2O.

Property	Value
Orbit Semi-Major Axis	0.01521 ± 0.00047 AU
Eccentricity	< 0.083
Stellar T_{eff}	2559 ± 50 K
Planet Mass	1.38 ± 0.61 $M_\oplus$
Planet Radius	1.056 ± 0.035 $R_\oplus$
Stellar Luminosity	-3.28 ± 0.03 $\log(L_\odot)$

Table 3: The basic properties of planet TRAPPIST-1c, that are used in the calculations done here. The data is taken from the Exoplanet Archive.

The planet is located at a distance of 0.01521 ± 0.00047 AU from its host star. A necessary condition for T_{eq} can be deduced to be $T_{\text{eq}} > 273.15$ K, which is the freezing point of H_2O. As upper limit for the equilibrium temperature we can take the boiling temperature of H_2O, which is equal to 373.15 K. Considering another solvent results in the liquid range changing as well (see Table 1 in Subsection 2.1. As discussed in Section 2, these are the transition points for a standard pressure(which is the Earth's average sea-level pressure of 1 atm or 1.01325 bar), which will be assumed for the exoplanet as well. The equilibrium temperature has been calculated using Equation 3. The parameter taken as variable is the albedo. The Bond albedo represents the energy reflected from a planet for all wavelengths and all phase angles, hence is a determination of how much energy is reflected (and thus absorbed) by the planet. The values used can be seen in Table 4.

Bond Albedo	Note
0.00	
0.068	Mercury
0.11	Moon
0.25	Mars
0.306	Earth
0.4	Pluto
0.5	
0.6	
0.7	
0.77	Venus
0.9	
0.95	
0.98	
0.995	

Table 4: The used values for the Bond albedo in calculating the corresponding equilibrium temperatures for planet TRAPPIST-1 c, with the values accompanied by a note the specific planet's Bond albedo[5].

The Bond albedo values from Table 4 have been computed with the help of Equation 3 for the redistribution factor being equal to 2 and 4 respectively. The resulting equilibrium temperatures can be seen in in Table 5. The measurement uncertainties for the luminosity (which has a value equal to -3.28 ± 0.03 $\log(L_\odot)$ and the semi-major axis given in the Exoplanet Archive are used to calculate the measurement uncertainties in the equilibrium temperatures. This resulted in a measurement uncertainty in the equilibrium temperatures equal to $+1.65\%$ and -1.55%, for both the $f = 2$ and the $f = 4$ case. The limitations in the concept of equilibrium temperatures (as discussed in the section before) result in systematic uncertainties that are significantly larger than the measurement uncertainties, implying that consideration of the measurement uncertainties is not necessary. Figure 4 displays the calculated equilibrium temperatures for the planet TRAPPIST-1c. The temperature boundaries of the different solvents are also displayed in the figure, with for example the green area representing the temperature range capable of supporting the presence of liquid H_2O.

[5]Planet albedos and mean surface temperatures via: https://nssdc.gsfc.nasa.gov/planetary/factsheet/

Bond Albedo	T_{eq} for $f = 4$ [K]	T_{eq} for $f = 2$ [K]
0.00	341.8	406.5
0.068	335.9	399.4
0.11	332.0	394.8
0.25	318.1	378.3
0.306	312.0	371.0
0.4	300.9	357.8
0.5	287.4	341.8
0.6	271.9	323.3
0.7	253.0	300.9
0.77	236.7	281.6
0.9	192.2	228.6
0.95	161.6	192.2
0.98	128.6	152.9
0.995	90.9	108.1

Table 5: The calculated equilibrium temperatures using different albedo values for TRAPPIST-1 c, with the corresponding redistribution factor included.

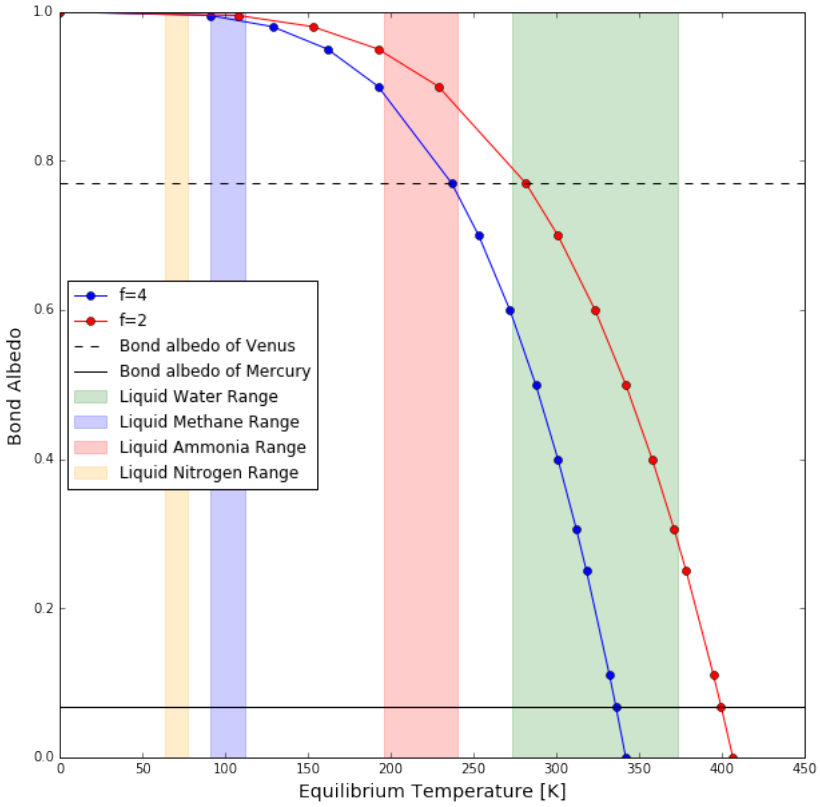

Figure 4: The equilibrium temperature of TRAPPIST-1 c for different albedo values and different values of the redistribution factor f. The temperatures inside the green area (ranging from 273.15 to 373.15 K) are able to support the presence of liquid H_2O, the yellow, blue and orange support liquid CH_4, NH_3 and N_2 respectively.

From Table 5 and Figure 4 it is seen that TRAPPIST-1 c seems to be a proper candidate for the support of liquid H_2O, by looking at its equilibrium temperature. For a redistribution factor equal to $f = 4$, it has the ability to support liquid H_2O with a Bond albedo ranging between 0 and 0.6. If the redistribution factor is taken as $f = 2$ the planet might be able to support liquid H_2O if it has a Bond albedo ranging from 0.3 to 0.8. In order to be able to support the existence of large amounts of liquid CH_4 or N_2 the planet would need a very high value for the Bond albedo of at least 0.97. Hence, without some other strong cooling mechanism on the planet this possibility can be excluded. If it however has a Bond albedo comparable to Venus for $f = 4$, it might be able to support the existence of liquid NH_3. These equilibrium temperatures and hence the ranges of Bond albedo values are however deduced under highly simplified conditions, which means that the actual surface temperature could be very different from what is calculated here, as is also seen from the discussion of $T_{/rmeq}$ for the Solar planets in Subsection 3.2. What is seen from Figure 4 is that for the redistribution factor being equal to 2 the equilibrium temperature is a factor 1.19 larger for all albedo values. Hence a planet that has redistribution of heat only at the hemisphere that faces its host star has a higher temperature than a planet with total planetary redistribution.

3.4 The equilibrium temperature for other exoplanets

Using the same method for the calculation of equilibrium temperatures, hence calculation via Equation 3, T_{eq} has been calculated for 599 exoplanets. The fact that the other $\pm$2900 exoplanets are missing is due to values for the stellar luminosity not being given in the Archive, since it only contains the luminosities for these 599 planetary systems. This thesis does however exceed the 418 known equilibrium temperatures in the Exoplanet Archive, since not all values have been calculated in the database. The temperatures have again been calculated as function of the Bond albedo, using the values as shown in Table 4. Figure 5 shows all the equilibrium temperatures as a function of semi-major axis, with the different albedo values indicated as well. In this figure only the temperatures with a redistribution factor $f = 4$ have been computed, since adjusting the factor to $f = 2$ will only imply a variation by a factor of 1.19, as can be seen from Figure 4.

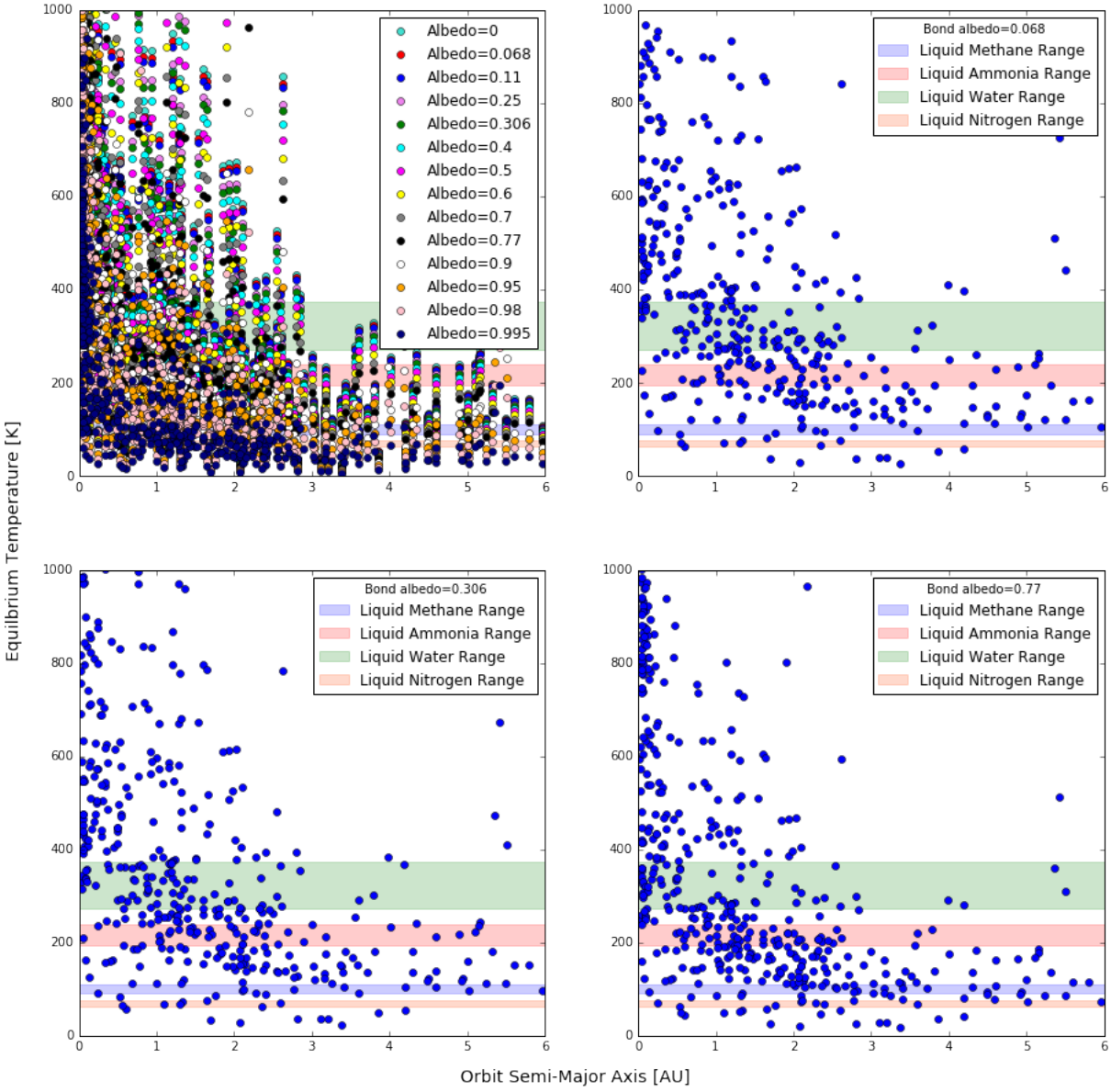

Figure 5: Equilbrium temperatures of exoplanets as function of the orbit semi-major axis, for different values of the Bond albedo. In the top-left figure all values for the Bond albedo as described in Table 4 are shown. In the top-right, bottom-left and bottom-right figures the equilibrium temperatures are shown for Mercury's Bond albedo, Earth's Bond albedo and Venus' Bond albedo values respectively. The blue, red, green and orange patches are indicating the range in which respectively CH_4, NH_3, H_2O and N_2 can be in the liquid phase. The redistribution factor f has been put equal to 4.

From Figure 5 it is seen that a higher value for the Bond albedo will lead to a lower value of the equilibrium temperature. For each of the values of the Bond albedo the number of planets that can support one of the solvents being in the liquid phase is shown in Table 7. The table also gives the associated percentage of the total, with the total being the 599 exoplanets for which the equilibrium temperatures are calculated. From this table it can be concluded that there are planets supporting the existence of liquid H_2O for almost every Bond albedo, since the temperature range for liquid H_2O is wide and consists of high temperatures. Liquid CH_4 and N_2 will need a high albedo, since a low temperature is needed for them being liquids. Planets in the liquid NH_3 range are quite abundant, for the same reasons as for H_2O. It can also be seen that when the only heating mechanism

Table 6: My caption

Bond Albedo	H_2O		CH_4		NH_3		N_2	
	Number	Percentage	Number	Percentage	Number	Percentage	Number	Percentage
0.00	61	10.2%	2	0.3%	25	4.2%	3	0.5%
0.068	58	9.7%	2	0.3%	28	4.7%	3	0.5%
0.11	59	9.8%	2	0.3%	30	5.0%	3	0.5%
0.25	58	9.7%	3	0.5%	32	5.3%	3	0.5%
0.306	57	9.5%	4	0.7%	32	5.3%	2	0.3%
0.4	61	10.2%	5	0.8%	35	5.8%	1	0.2%
0.5	65	10.9%	6	1.0%	37	6.2%	2	0.3%
0.6	69	11.5%	7	1.2%	37	6.2%	1	0.2%
0.7	74	12.4%	8	1.3%	37	6.2%	1	0.2%
0.77	76	12.7%	9	1.5%	38	6.3%	2	0.3%
0.9	75	12.5%	21	3.5%	39	6.5%	7	1.2%
0.95	54	9.0%	26	4.3%	55	9.2%	11	1.8%
0.98	56	9.3%	40	6.7%	47	7.8%	22	3.7%
0.995	71	11.9%	44	7.3%	33	5.5%	40	6.7%

Table 7: The number of planets with equilibrium temperatures lying in each of the different liquid ranges, for the different values of the Bond albedo, with the percentage of the total 599 known equilibrium temperatures.

that is being considered is the incoming energy from the host star most of the planets seem to be unable to support the existence of liquid H_2O. For a higher albedo value more planets will decrease in temperature towards the liquid NH_3 or even the liquid CH_4 or N_2 range, as can be seen in the four figures shown in Figure 5. H_2O as a solvent results in the largest number of planets for most albedo values, since it has the biggest temperature range of the solvents. Another reason for H_2O being the most favorable solvent is the fact that most chemical reactions, which are essential for life, are more likely to happen at higher temperatures. Again however it should be noted that the equilibrium temperature is only a rough estimation of the true surface temperature. For example planets below the liquid H_2O range could have other heating mechanisms that makes their temperatures rise up to the range that supports liquid H_2O. The concept of the appropriate equilibrium temperatures leads to the concept of the so-called Habitable Zone.

4 Effective Atmosphere and Habitable Zone

This section will discuss the concept of the Habitable Zone and atmospheric influence on it, for the specific case of the TRAPPIST-1 system. It will start with some values found for the Solar HZ in Subsection 4.1 and some important definitions regarding the effective atmosphere. Then the HZ boundaries are calculated for the TRAPPIST-1 system in Subsection 4.2. Subsection 4.3 contains a discussion about the influence of CO_2 on the HZ boundaries.

4.1 HZ boundaries

The Habitable Zone is the zone around a star in which planets are able to support the presence of liquid H_2O, given sufficient atmospheric pressure. Since using a different solvent will adjust the temperatures in which a planet might be considered habitable, Neubauer et al. proposed a new concept called Life Supporting Zones (LSZ) (Neubauer et al., 2011). The discussion done in this section will be limited to only the H_2O-based HZ, with a focus on the influence of albedo and greenhouse gases. The influence of albedo will be comparable when using another solvent, while not much is known for the CO_2 influence in planetary environments based on another solvent.
The first estimates of the Solar HZ boundaries are found by calculations in a 1-D climate model by Kasting et al. (Kasting et al., 1993). In this model, the inner edge is determined as the distance at which the planet experiences a runaway greenhouse effect: the positive feedback between the surface temperature and atmospheric opacity will lead to an increase in temperature that is uncontrollable (Kopparapu et al., 2016). This results in the complete evaporation of the H_2O in-

ventory and the planet will hereby lose its H_2O inventory via photolysis and Hydrogen escape. Another way of calculating the inner edge of the HZ is to consider the moist greenhouse, in which there is a continuous but slower increase in the H_2O vapor content of the atmosphere, which will again lead to loss of Hydrogen after the dissociation of H_2O (Kopparapu et al., 2016). The outer edge is determined by the maximum greenhouse effect, also known as the distance at which addition of CO_2 to the atmosphere will not be sufficient anymore to heat up the surface above the freezing point. In fact it will lead to a decrease in temperature, since CO_2 increases the planetary albedo (Kasting et al., 1993). The edges of the HZ are dependent on the stellar flux and hence are different in each stellar system. According to Kasting et al., the Solar HZ stretches from 0.95 AU (moist greenhouse) or 0.84 AU (runaway greenhouse) out to 1.67 AU. Kopparapu et al. (Kopparapu et al., 2013) stated an updated version of the Habitable Zone, with an inner edge equal to 0.97 AU for the runaway greenhouse limit and 0.99 AU for the moist greenhouse limit, and an outer edge of 1.688 AU. These new estimates are based on better models of the runaway greenhouse effect and H_2O loss effects. This means that Earth is at the inner edge and thus close to the runaway greenhouse effect (Kopparapu et al., 2013). Hence it can be noted that the boundaries of the HZ are strongly related to the influences that a planetary atmosphere has on the incoming energy, both in letting it through as well as retaining the energy. Assuming an atmosphere, the HZ edges are also dependent on the spectral type of the host star, since each type produces another wavelength range as output (Kopparapu et al., 2013). For an F-star the planetary albedo will be higher than for an M-star, since an F-star shines more towards the blue and hence the cross section for Rayleigh scattering is higher ($\propto \frac{1}{\lambda^4}$). In addition, gases such as CO_2 have higher absorption in the near-infrared than in the visible, and therefore more stellar radiation is absorbed for a redder star (M-type). As a result of stellar evolution, the boundaries of the HZ will change as time passes by.

4.2 Calculation of HZ: planet TRAPPIST-1 c

Since the boundaries of the Habitable Zone are defined as the temperatures at which H_2O will leave the liquid phase, these boundaries can be calculated for the planetary system TRAPPIST-1 by writing Equation 3 into an equation for the distance to the host star:

$$a = \left(\frac{L_{star} * (1 - A)}{4\pi f \sigma T^4}\right)^{1/2} \qquad [\text{m}] \qquad (4)$$

Inserting the freezing and boiling temperatures of H_2O and conversion to AU will lead to values for the outer and inner boundary of the HZ respectively. From Equation 4 it is seen that also the boundaries of the Habitable Zone depend on the planetary albedo. Thus, using Equation 4 the boundaries for the albedo values found in Table 4 have been calculated. The resulting boundaries are shown in Figure 6.

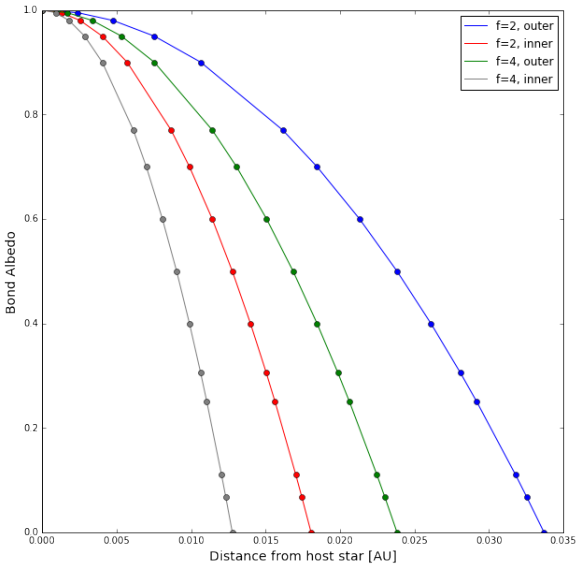

Figure 6: The correlation between the outer and inner boundaries of the HZ and the value of the albedo effect for the planetary system TRAPPIST-1, for different values of the redistribution factor.

From Figure 6 we see that for a higher albedo, the inner and outer boundaries of the HZ lie closer towards the host star. This is as expected, since a higher albedo means that more stellar energy is being reflected and hence the planetary environment will be colder: it needs to be closer to the host star in order to be habitable. Next to that it can be seen that the boundaries are closer to the host star for $f = 4$. This is also as expected since this redistribution factor results in a lower planetary equilibrium temperature, as has been discussed in Section 3. By considering albedo's comparable to Mercury, Earth and Venus the HZ boundaries shown in Table 8 have been found. The measurement uncertainties for the HZ boundaries can also be calculated by taking into account the uncertainty in the stellar luminosity. For the

inner boundaries this results in measurement uncertainties of +3.33% and −3.16%, and for the outer boundaries +3.28% and −3.16%. This is for both values of the redistribution factor. Again we can conclude that the systematic errors are much larger than the measurement errors, mainly because of assumptions about the atmospheric influence on the HZ boundaries. In order to make a qualitative statement about these systematic errors, more information about the specific atmospheric properties should be known.

	f=4		f=2	
Bond Albedo	Inner boundary[AU]	Outer boundary[AU]	Inner boundary[AU]	Outer boundary[AU]
0.068	0.012	0.023	0.017	0.033
0.306	0.011	0.020	0.015	0.028
0.77	0.006	0.011	0.009	0.016

Table 8: The boundaries for the planetary system TRAPPIST-1 corresponding to temperatures in which H_2O can still be in the liquid phase. The boundaries have been calculated for different albedo's and redistribution factors.

4.3 The influence of CO_2 on HZ boundaries

As stated in Subsection 2.3, CO_2 can be considered as an important greenhouse gas. Therefore the influence of it on the HZ boundaries will need discussion in some more detail. Since the inner boundary based on the runaway greenhouse effect is determined as the point at which a planet's H_2O inventory is completely vaporized and hence will escape to outer space, one can make the assumption that an atmosphere experiencing the runaway greenhouse effect is H_2O dominated (Kopparapu et al., 2013) (Kopparapu et al.). Therefore, increasing the amount of CO_2 and hence the atmospheric pressure will not influence the inner boundary when it is calculated in this way. Since determination via the moist greenhouse effect is the slower effect and is dependent on the amount of H_2O vapor in the atmosphere, an increase in CO_2 pressure will lead to a higher surface temperature and hence in more evaporation of H_2O. But again, the atmosphere will already be H_2O dominated. The outer HZ boundary is however totally dependent on the amount of CO_2, since a planetary atmosphere located here is already CO_2 dominated (Kopparapu et al.). The boundaries are dependent on the effective stellar flux that is reaching the planet. This dimensionless effective flux can be written as:

$$S_{eff} = \frac{F_{IR}}{F_*} \tag{5}$$

In this equation F_{IR} is the outgoing infrared radiation at the top of the atmosphere and F_* is the incoming stellar radiation at the same location (Kopparapu et al., 2013). As one increases the CO_2 pressure in a CO_2 dominated atmosphere, F_{IR} decreases initially and F_* decreases as well due to Rayleigh scattering (and thus an increasing albedo). From a value of ± 10 bar CO_2, F_{IR} will become constant due to the atmosphere becoming optically thick. Then Rayleigh scattering by CO_2 will balance and eventually outweigh the greenhouse effect. The combination of these effects will lead to a minimum effective flux at a CO_2 pressure of ± 8 bar, which is what we know as the maximum greenhouse (Kopparapu et al., 2013). The effect of the greenhouse gas on the effective stellar flux is described by a parametric fit proposed by Ludwig et al. (Ludwig et al., 2016):

$$S_{eff} = S_{eff,\odot} + aT_* + bT_*^2 \tag{6}$$

In this equation, $S_{eff,\odot}$ is a fit parameter for the effective solar flux at the specific location. The factors a and b are also fit parameters, based on the absorption coefficients of H_2O and CO_2 and adapted from the HITEMP database (Ludwig et al., 2016).

Constant	1bar CO_2 OHZ	8bar CO_2 OHZ
$S_{eff,\odot}$	0.6774	0.4597
a [K^{-1}]	$3.3998 * 10^{-5}$	6.7254^{-5}
b [K^{-2}]	1.0272^{-8}	$3.3246 * 10^{-9}$

Table 9: The values for the fit parameters in the calculation of the stellar effective flux, for a different atmospheric CO_2 pressure. From Ludwig et al. (Ludwig et al., 2016)

The calculated stellar effective flux from Equation 6 can be converted in the distance of the HZ boundary via:

$$d = (\frac{L/L_\odot}{S_{eff}})^{0.5} AU \tag{7}$$

This calculation has been performed on the planet TRAPPIST-1c, giving an outer HZ boundary equal to 0.028 ± 0.001 AU for an 1bar CO_2 dominated atmosphere and equal to $0.045^{+0.002}_{-0.001}$ AU for an 8bar CO_2 dominated atmosphere. Hence we can see that an increase of CO_2 pressure from a 1 bar to 8 bar results in an extension of the outer HZ boundary 1.6 times farther out, corresponding to a temperature change of 27%. The advantage in calculating HZ boundaries in this way is that the effect of greenhouse gases is taken into account, which calculation via the Bond Albedo does not. One will however need the different factors and information about the abundances of greenhouse gases.

The influence of the CO_2 pressure on the Solar System HZ can also be calculated, using the luminosity and effective temperature of the Sun (5772 K)[6]. For a 1 and 8 bar CO_2 pressure this results in the outer HZ being at 1.215 and 1.475 AU respectively. Hence Mars, which is located at a distance of 1.52 AU from the Sun, would have been close to the outer edge of the HZ if its CO_2 pressure would be around 8 bar. The pressures considered can be compared to Solar planets that have a surface pressure that is known. For Venus, Earth and Mars this surface pressure is 92 bar, 1.01325 bar and $6 - 9$ mbar respectively[7]. This pressure can be used since it is the atmospheric pressure on a surface point. Next to that, it is known that Mars and Venus have CO_2 dominated atmospheres, with a CO_2 fraction of 96% and 96.5% respectively [Rauf et al., 2015]. For Earth this is different, since its atmosphere only contains a CO_2 fraction of 0.04%. Even though the Martian atmosphere is thus CO_2 dominated, the surface is still cold because of its large distance to the Sun and above that due to the atmosphere being very thin, as can also be seen from the low Martian surface pressure. For Venus, the amount of CO_2 actually plays a major role in ruling its climate. As seen from the high surface pressure, the atmosphere on Venus is dense and thick, resulting in a high surface temperature (737K) due to the strong greenhouse effect here. Hence, especially for Venus the outer HZ boundary would extend outwards due to the CO_2 fraction in its atmosphere.

5 Eccentricity of exoplanets orbits

This section will discuss the criteria of a maximum eccentricity for orbits of exoplanets. It starts with an introduction of exoplanet eccentricities. Subsection 5.2 determines a maximum eccentricity using the TRAPPIST-1 system, which is afterwards applied to other exoplanets in Subsection 5.3.

5.1 Distribution of eccentricities

The known values for the eccentricities are seen in Figure 7. From this figure it is seen that the exoplanet eccentricities over the range from 0 to 1 are similar in comparison to our Solar System, of which the inner planet eccentricities are also shown. The maximum orbital eccentricity for Solar System planets is Mercury's 0.205, while a minority of exoplanets exist with eccentricity values of $e > 0.3$. This could be either due to an unusual formation history, or due to a special structure of the stellar system. In the Solar System Jupiter plays a big role in establishing the eccentricity values(O'Brien et al., 2014), but this could be very different for other stellar systems and has to be researched for each system separately.

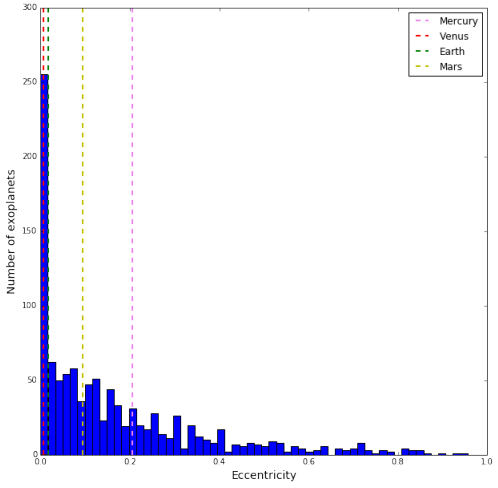

Figure 7: Eccentricities that are known so far, with the lines indicating the eccentricities of several Solar planets.

5.2 TRAPPIST-1c

In order to see whether a planet with a certain eccentricity is still habitable, a new condition can be deduced that has to be satisfied by the planet:

[6]Via the NASA Sun fact sheet: https://nssdc.gsfc.nasa.gov/planetary/factsheet/sunfact.html
[7]Values via NASA planetary fact sheet: https://nssdc.gsfc.nasa.gov/planetary

the eccentricity of a planet must be small enough to prevent the planet's orbit from exceeding the boundaries of the Habitable Zone. For planet TRAPPIST-1c these inner and outer boundaries of the Habitable Zone, which are shown in Table 8, can be used to put a limit on the eccentricity of the planet's orbit. By using the outer boundary as the semi-major axis a and the inner boundary as the semi-minor axis b the maximum eccentricity e_{max} can be calculated via:

$$e_{max} = \sqrt{1 - \frac{b^2}{a^2}} \tag{8}$$

Whatever value used for the albedo of a planet, the ratio between the inner and outer boundary will stay the same and hence the maximum eccentricity will have the same value as well. Since the ratio also cancels the influence of the stellar luminosity, the maximum eccentricity will be same for every stellar system. Using the TRAPPIST-1 values of the HZ, the maximum eccentricity is given by 0.844 when H_2O is used as a solvent. This value must be used with caution however, since it is the eccentricity associated with a planet that lies exactly in the middle of the Habitable Zone. Therefore, a planet situated closer to one of the boundaries would need a smaller eccentricity. Next to that, as can be seen in Table 8, the HZ boundaries are dependent on the albedo value of the planet. Since the eccentricity of TRAPPIST-1c is < 0.083 and its semi-major axis is given by 0.01521 ± 0.00047AU[8], we conclude from Figure 4 and Table 8 that this planet will stay in the Habitable Zone of its host star during the orbit around it, if it has a redistribution factor $f = 4$ as long as its albedo is not larger than 0.6. For the factor being equal to 2, we can conclude it will be located inside the HZ for an albedo value $0.31 < A < 0.8$, and hence it can only be considered to have a habitable eccentricity when its albedo is in this range.

5.3 Eccentricity limits for other solvents

To expand the discussion about habitable eccentricities to other exoplanets, the boundaries of the associated HZ's can be calculated again via Equation 4. Since calculating the maximum eccentricity via Equation 8 however takes the fraction of the inner and outer boundary of the HZ and removes the dependence on stellar luminosity, this maximum eccentricity will stay the same no matter what planet is considered. The maximum eccentricity will however be different if different solvents are considered for the support of life on a planet. Hence we use Equation 4 again and insert the freezing and boiling temperatures of solvents shown in Table 1. The resulting maximum eccentricities are shown in Table 10. From the table also the number of planets satisfying the maximum eccentricity condition can be seen. Since the eccentricities are only known for 1068 of the known exoplanets[8] , we can conclude that by ignoring their exact location between boundaries, most of the planets are satisfying the conditions that limit the value of eccentricity. In the discussion following later, the exact location of the planets inside the boundaries will be calculated and discussed in order to see whether the planets will really stay inside the boundaries.

Solvent	Max eccentricity	Number of Planets	Percentage of total
H_2O	0.844	1061	99.3%
CH_4	0.752	1049	98.2%
NH_3	0.748	1049	98.2%
N_2	0.746	1049	98.2%

Table 10: The maximum eccentricities for the different solvents to keep a planet inside the boundaries of their HZ and the number of planets that satisfy these maximum eccentricities. It should however be noted that this maximum eccentricity is associated with a planet that is located exactly in the middle between the boundaries.

[8]from the NASA exoplanet archive: https://exoplanetarchive.ipac.caltech.edu/index.html

6 State of planetary surface

As mentioned in Subsection 2.6, another condition for having a habitable planet is the existence of a solid or a liquid surface. It is however not straightforward to getting limits in between which a planet can be seen as rocky: hence composed of metals and having a solid surface. This section first reviews some theories about planetary mass and radius limits in Subsection 6.1 and after that these theories are applied to the planets in the database.

6.1 Mass and radius limits

Theories about the planetary mass tell us that masses should not exceed a value of $10M_\oplus$ in order not to become a gas or ice giant (Mizuno et al., 1978) (Ida and Lin, 2004). That this value is approximately true is seen in Figure 8. This figure shows that for masses lower than $10M_\oplus$ the density is roughly constant with increasing mass. However, after a mass of $10M_\oplus$ the density decreases with increasing mass. From this mass the planet starts to attract large amounts of volatiles, such as H and He. Therefore, even though the mass increases, the average density will be lower and the planet will become a gas or ice giant.

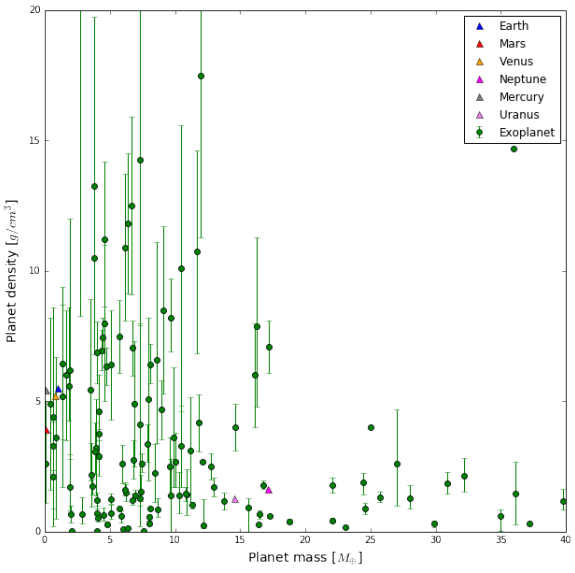

Figure 8: Exoplanet mass versus density. Also the Solar System planets that have masses within the mass range are included[9]. A change in density behaviour as function of mass can be seen around a mass of $10M_\oplus$.

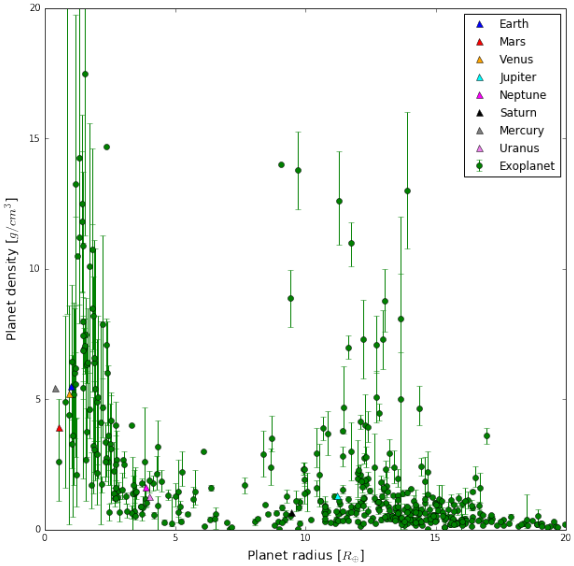

Figure 9: Exoplanet radius versus density. Also the Solar System planets are included[9]. A change in density behavior as function of radius can be seen around a radius value of $2R_\oplus$.

A similar limit has been deduced for the radii of rocky exoplanets, which constrains the radius to be smaller than a value of $2R_\oplus$ (Weiss and Marcy, 2014) (Seager et al., 2007). Figure 9 displays this theory, showing that there is also a change in density behavior as function of radius, around a value for the radius of $2R_\oplus$. With the same reasoning we can conclude that planets exceeding this value attract large amounts of volatiles, lowering the average density and turning them into gas or ice giants. Looking at the planets in the Solar System, which are plotted as the colored triangles in the figures 8 and 9, it can be seen that the limits for the planetary mass and radius are satisfied. Figure 9 misses the values of Jupiter and Saturn since their masses are exceeding the range of this figure (317.83 $M_\oplus$ and 95.16 $M_\oplus$ respectively[9]). We see that the four inner planets satisfy both $M_P < 10M_\oplus$ as well as $R_P < 2R_\oplus$ and are indeed proven to have a solid surface, while the outer planets do not satisfy these criteria and are indeed found to be gas or ice giants. From the Solar planet density values, we can deduce a lower density limit of solid planets to be around 3 g/cm^3. Although the limiting mass and radius values from these theories are somewhat robust, they are satisfied by the Solar System and can be used as upper limit for the presence of a solid surface. As discussed in section 2, theories exist for a lower limit for the planetary

[9]Planet values via NASA planetary fact sheet: https://nssdc.gsfc.nasa.gov/planetary

mass to be taken as $0.3M_{\oplus}$. Because evidence in our Solar System is not in agreement with this theory, it will not be taken into consideration.
Figure 10 shows a plot of the mass versus the radius of the known exoplanets. The planetary mass is given for only 674 of the exoplanets, since measuring the true mass is difficult and often a combination of both the transit and radial velocity detection methods are needed for it. The radius is known for 2763 planets, so the limiting factor in this discussion is the mass. The shaded area represents the planets that are able to support a solid surface, according to the theories mentioned above. It can again be seen that the Solar System planets fit into the theories: the outer four planets have both a radius and a mass that is too big to have a solid surface and hence are gas or ice giants. The inner four planets fall inside the appropriate range and indeed are found to have a solid surface.

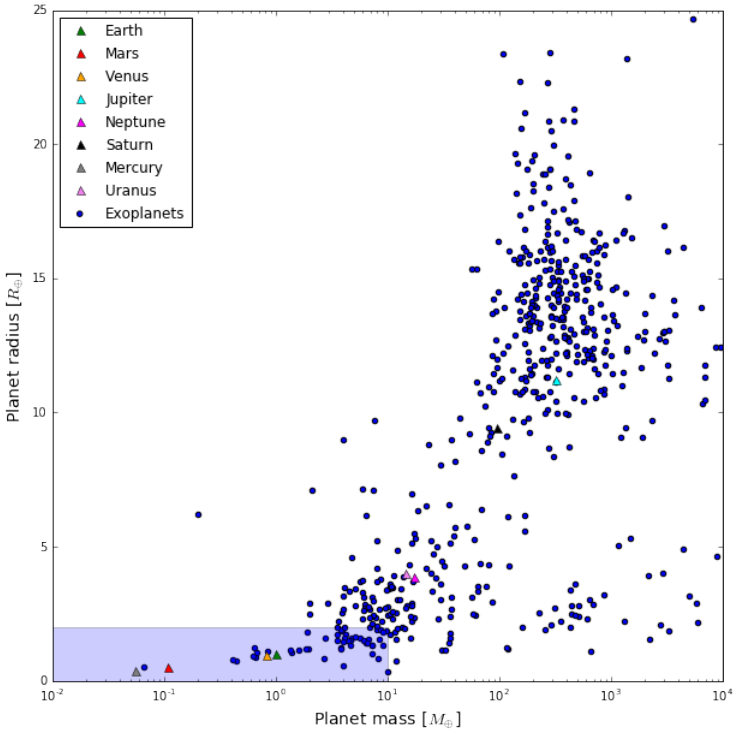

Figure 10: Exoplanet mass versus radius. The Solar System planets are included, with their data taken from NASA. The shaded area represents the ranges of masses and radii that can be seen as being able to have a solid surface.

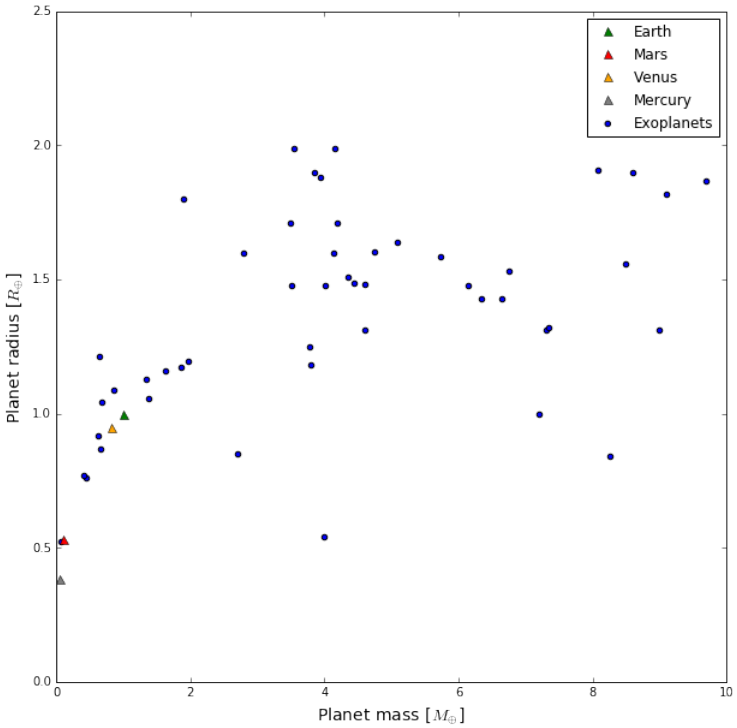

Figure 11: Exoplanet mass versus radius for the habitable ranges of radii and masses.

Figure 11 shows the 49 planets left that are able to have a solid surface according to the data and the theories mentioned above. This a fraction of only 7.2% of the total (with mass and radius known) being able to provide a solid surface. It should however be mentioned that this fact also arises because of observational limitations. Detections of exoplanets involve mostly the larger planets, since the smaller (and probably more favorable for emergence of life) planets are harder to detect.

In addition, even the planets found in the appropriate ranges could still be uninhabitable, since an exoplanet surface can only be proven to be habitable with the use of surface sensitive observations (Robinson, 2017). For example, from the discussion in this section and the equilibrium temperature calculation done in Subsection 3.2 Venus might be considered to be able to provide a habitable environment. The discussion in Subsection 4.3 however describes the influence of its atmosphere in excluding this possibility.

Albedo	H_2O planets	CH_4 planets	NH_3 planets	N_2 planets
0.068	TRAPPIST-1 c TRAPPIST-1 d		TRAPPIST-1 f LHS 1140 b	
0.306	TRAPPIST-1 b TRAPPIST-1 c		LHS 1140 b TRAPPIST-1 e TRAPPIST-1 f	
0.77	TRAPPIST-1 b HD 219134 f		TRAPPIST-1 c TRAPPIST-1 d	
0.9	HD 219134 f Kepler-62 c	TRAPPIST-1 g	TRAPPIST-1 b	

Table 11: Habitable planets according to their mass, radius and equilibrium temperature characterized by different values for the Bond albedo. The planets are represented by their host star and their own planet letter.

Planet	Eccentricity	Orbit SMA
TRAPPIST-1 b	< 0.081	0.0111 ± 0.0003
TRAPPIST-1 c	< 0.083	0.0152 ± 0.0005
TRAPPIST-1 d	< 0.070	0.0214 ± 0.0006
TRAPPIST-1 e	< 0.085	0.0282 ± 0.0008
TRAPPIST-1 f	< 0.063	0.0371 ± 0.0011
TRAPPIST-1 g	< 0.061	0.0451 ± 0.0014
HD 219134 f	0.148 ± 0.047	0.1463 ± 0.0018
Kepler-62 c		0.093 ± 0.001
LHS 1140 b	< 0.29	0.088 ± 0.004

Table 12: The known eccentricities and orbit semi-major axes for the planets that fulfill all the criteria.

7 Discussion

Subsection 7.1 puts together the results that are found in Sections 3 up to and including 6. This is done by checking whether there are planets having an appropriate equilibrium temperature as discussed in Section 3 as well as radius and mass below the upper limit as described in Section 6. The total number of planets that have both their equilibrium temperatures as well as mass and radius known is 567. After this the planetary eccentricities are combined with the HZ boundaries, in order to ensure that the leftover planets will stay in the corresponding HZ during their orbit. Subsection 7.2 contains a comparison of the possible habitable planets with literature.

7.1 Combining the criteria

The planets that might be considered habitable can be found by combining the ranges for planetary mass and radius with the appropriate temperature ranges for the different solvents. The resulting planets id's are listed in Table 11, hence we end up with 9 planets out of 567 that might contain a habitable environment (which is a percentage of 1.6%). To see that these results are indeed true, they can be compared to Figure 4 for planet TRAPPIST-1c.
We consider albedo values up to 0.9, since values exceeding 0.9 would need more reflection than seems realistic. As stated in Section 5, another condition for a planet to be habitable is that its eccentricity does not exceed a maximum value. These maximum values are dependent on the solvent considered on the planet and can be seen in Table 10. In order to see whether the planets that might be habitable satisfy these constraints we have to use their eccentricity values. The eccentricities are shown in Table 12, together with the values for the semi-major axes of the different planets. If we only look at the eccentricities, we see that all planets have their eccentricity value inside the range that might be considered habitable for the different solvents. Only for planet Kepler-62c the eccentricity is not known, so before one can say anything about this planet its eccentricity should be known first.

Looking at the TRAPPIST-1 system, some boundaries for its liquid H_2O HZ have already been calculated in Section 4. The HZ boundaries per Bond albedo value can be combined with the eccentricities and the semi-major axes of planetary orbits that might be habitable using H_2O as a solvent. As discussed in Subsection 4.3, the amount of CO_2 makes a large difference in where the outer limit of the HZ is situated. Nonetheless, the HZ calculations here will only be based on the Bond albedo value. This is because the Bond albedo is a well known range consisting of all possible reflections. The parameters known for the CO_2 influence are limited and leave out the influence of other greenhouse gases as well. Doing the HZ calculations it can be deduced whether these planets indeed stay inside the HZ boundaries and hence will be able to support the existence of life using H_2O as a solvent. Only a planet with a semi-major axis located close to the inner boundary of the HZ might lead to the planet exceeding the boundary when its semi-minor axis is located outside the HZ. The HZ boundaries will only be calculated for a redistribution factor $f = 4$, since the effect of adjusting the factor to $f = 2$ is small enough to ignore, as discussed in Subsection 4.1. The calculated HZ boundaries for the habitable systems can be seen in Table 13. The measurement uncertainties are calculated from the uncertainties given in the Exoplanet Archive, and are negligible compared to the systematic uncertainties, because of assumptions made about for example the atmospheric influence. The resulting measurement uncertainties in the HZ boundaries are $+3.28\%$, -3.16% for the TRAPPIST-1 system, $+0.95\%$, -0.94% for the HD 219134 system, $+3.61\%$, -3.51% for the LHS 1140 system and

+4.83%, −4.71% for the Kepler-62 system.

The Bond albedo equal to 0.068 leads to planets TRAPPIST-1c and d being in the sufficient temperature range to support liquid H_2O. From Tables 12 and 13 we then see that both planets are indeed inside the HZ boundaries. Planet c is located towards the middle of the HZ, while planet d is more towards the outer edge of the HZ. Besides that both planets have a small eccentricity, resulting in an almost circular orbit and keeping them inside the HZ boundaries for their entire orbit. For an Earth-like Bond albedo of 0.306 the planets TRAPPIST-1b and c have the right temperatures. Planet c is again located in the middle of the HZ and will stay inside it for its orbit because of its small eccentricity. Planet b however is located just inside the HZ, laying very close to the inner edge. Hence even though the planet has a small eccentricity, it may exceed the inner boundary partly during its orbit. Its semi-minor axis b can be calculated by rewriting Equation 8 to:

$$b = a(1 - e^2)^{1/2} \tag{9}$$

This results in a semi-minor axis for planet TRAPPIST-1b equal to ±0.01106 AU. Hence the planet will stay close to the inner edge, but still inside the HZ. A Venus-like Bond albedo of 0.77 will again lead to habitable temperatures for planet b. In this case however, the planet is located close to the outer edge of the HZ, and therefore the planet will again stay inside the HZ for its entire orbit. The other planet having the right liquid H_2O temperature for this albedo is HD 219134f. This planet is located appropriately inside the HZ. For a high albedo of 0.9 this is the same for HD 219134f, and hence it will stay in the HZ during its orbit in both cases. For Kepler-62c and an albedo of 0.9 we can see that its semi-major axis fits inside the HZ of the system. However, since there is no eccentricity known, it cannot be said whether the planet will stay inside the HZ and hence will be capable to support life. When using liquid CH_4 as a solvent, so far only one planet is found following the criteria, namely TRAPPIST-1c. This planet is located at the inner edge of the HZ for CH_4 around the host star with the semi-minor axis calculated to be ±0.0450 AU. Hence also TRAPPIST-1c will stay at the location of the inner edge, but still inside the HZ.

Stellar system and solvent		Albedo			
		0.068	0.306	0.77	0.9
TRAPPIST 1: H_2O	inner HZ [AU]	0.012	0.011	0.006	0.004
	outer HZ [AU]	0.023	0.020	0.011	0.008
TRAPPIST 1: CH_4	inner HZ [AU]	0.138	0.119	0.068	0.045
	outer HZ [AU]	0.209	0.180	0.104	0.068
TRAPPIST 1: NH_3	inner HZ [AU]	0.030	0.026	0.015	0.010
	outer HZ [AU]	0.045	0.039	0.022	0.015
HD 219134: H_2O	inner HZ [AU]	0.277	0.239	0.138	0.091
	outer HZ [AU]	0.517	0.446	0.257	0.169
LHS 1140: NH_3	inner HZ [AU]	0.071	0.061	0.035	0.023
	outer HZ [AU]	0.107	0.092	0.053	0.035
Kepler-62: H_2O	inner HZ [AU]	0.247	0.213	0.123	0.081
	outer HZ [AU]	0.460	0.400	0.229	0.151

Table 13: The inner and outer boundaries of the HZ, calculated using the boiling and freezing temperatures of the different solvents. The boundaries are shown for the different values of albedo's with which the habitable planets have been determined.

NH_3 considered as the solvent also results in most of the planets fitting appropriately between the computed ranges of the associated HZ. Only planets TRAPPIST-1b and c with a Bond albedo of 0.9 and 0.77 respectively are located close towards the inner boundary. However, since their eccentricity has a small value, none of the planets will exceed the inner HZ boundary. It should be stated that even when a planet exceeds the HZ boundaries because of an eccentric orbit, it might still be able to keep its surface temperature in the right temperature ranges. This can be achieved via mechanisms on the planet itself, for example geological activity or a thick atmosphere that retains the heat on the planet.

Combining all criteria results in the 9 planets shown in Table 11, which have been determined as having the right conditions: they are capable of having a solid or liquid surface, supporting the existence of one of the solvents discussed

here and they have an eccentricity small enough to keep them in their host star's HZ during the orbit. However, as already can be seen from the table, their habitability is dependent on the planetary albedo and hence on the atmospheric composition, cloud reflection and surface reflection. This could turn out to be very different than the assumptions done in this thesis. As discussed in Section 4, a difference in the atmospheric composition might result in different boundaries of the HZ and next to that a different planetary equilibrium temperature. Moreover, even though the planets can be considered capable of supporting the existence of a solvent, it still needs to have a sufficient amount of the solvent available. Hence it needs to have attained an initial inventory of volatiles somewhere in the past. The activity of the host stars should not be a problem, since the stars found with surrounding planets are all late-type stars, being even less luminous than the Sun[10]. The presence of geological activity might again lead to differences in planetary conditions from the calculations done here: for example it might lead to a much higher fraction of greenhouse gases. However, as stated before geological activity can also help a planet in stabilizing its surface temperature. The presence of a planetary magnetic field and the rate of planetary rotation could not be researched here, but a magnetic field might be able to provide necessary surface protection and planetary rotation could have a large influence on the surface temperature.

7.2 Comparison with literature

Several other planetary systems have been discussed as possibly hosting one or more habitable planets. Examples of those systems are Gliese-581 and Proxima Centauri (Selsis et al., 2007) (Turbet et al., 2016) (Ribas et al., 2016). The first of these is thought to include at least one planet, namely planet c, inside its HZ (Selsis et al., 2007). The fact that this planet is not included in the results is due to missing values for its mass and radius in the database. The minimum value of its mass is however given as 5.5 ± 0.3 $M_{\oplus}$. An update of the archive including the radius of $2.2 - 2.6$ $R_{\oplus}$ (Selsis et al., 2007) might result in an extra habitable planet via this thesis. The same incompleteness is the reason that the planet Proxima Centauri b, does not come out as a habitable planet in this thesis. For this planet the radius is not known at all (Ribas et al., 2016). The lack of these values is due to the planets being detected with the radial velocity method, which is described in Section 1.1. Other examples of interesting planets missing essential data include Kepler-186f (Quintana et al., 2014) and Kepler-138b (Jontof-Hutter et al., 2015). These planets are missing values for a mass and semi-major axis respectively. Earlier research on the TRAPPIST-1 system resulted in equilibrium temperatures for the planets b, c, d, e, f and g that can be considered habitable (Gillon et al., 2017) and is thus in agreement with the results in this thesis. The same can be said for the planets HD 219134f (Vogt et al., 2015) and Kepler-62 c (Borucki et al., 2013).

8 Conclusion

In this thesis research has been done on the habitability of exoplanets. Multiple criteria are involved in the determination whether a planet is habitable or not. Only a few of those criteria can already be applied on the planets available in the NASA exoplanet archive, including calculations of temperature, atmospheric influence, eccentricities and mass and radius. By applying these parameters on the 3486 planets known in the NASA exoplanet archive the nine planets shown in Table 11 are found to be capable of supporting the existence of the specific solvent. It should however be noted that this research is far from complete, since the database is lacking a lot of values of parameters that are certainly needed, e.g. luminosity or planetary mass. Due to this missing data, the 9 planets are out of a total of 567 that have the necessary parameters defined in the database, hence a percentage of 1.6%. From Table 11 we see that H_2O and NH_3 so far have the most favorable liquid temperature ranges in providing a habitable environment. The resulting planets should be considered with caution however, since their true temperature might be considerably different from the calculated equilibrium temperature.
It has been shown that changing the pressure of a CO_2 dominated planetary atmosphere from 1bar to 8bar leads to an extension in the outer HZ boundary of about 60%, and therefore has an influence of about 27% on the equilibrium temperature of a planet. Hence more information about atmospheric composition of planets and the influence on the planetary environment is needed. In addition to that, improvements and extensions of the CO_2 models would improve our knowledge about its influence.
Planet HD 219134f has been found via the ra-

[10] Spectral types can be found on SIMBAD astronomical database http://simbad.u-strasbg.fr/simbad/ or in the exoplanet archive.

dial velocity method, while the other eight planets have been found via the transit method. The transit method at the moment seems to be the most favorable in finding habitable exoplanets, since it has the capability of finding relatively small planets in an Earth-like orbit around the star. The problem with the method is however that the probability of a transit in the line-of-sight is small. Especially the radial velocity and microlensing method are dependent on the gravitational pull of planets, and hence are more likely to find bigger planets.

9 Outlook

As a future goal, gathering more knowledge about exoplanet atmospheres is a priority in the determination of habitable environments. Next to that, the search should be adjusted in order to find more terrestrial planets. Hence this would mean smaller planets, capable of sustaining a solid surface. While transit and radial velocity are still delivering most of the exoplanet discoveries, direct imaging might be the future, having the capability of finding planets at larger orbits. This might hence lead to more planets in the temperature range of liquid CH_4 or N_2, or big H_2O planets around a luminous host star. Moreover, direct imaging can also lead to spectra, which can be studied in order to research atmospheric composition. Some transit spectra of exoplanets do already exist, an example of this is planet HD 209458b (Swain et al., 2009). This spectra does show signs of CH_4 and H_2O and CO_2.
The future of the search for exoplanets does however seem to be bright. The launch of the James Webb Space Telescope (JWST)[11] in 2018 might lead to new exoplanet discoveries using the direct imaging as well as the transit method. This telescope will also be used to study exoplanet atmospheres, in the hope of finding a similar one to Earth. Since this telescope is however launched with a variety of different goals, it will only have a limited time available to search for exoplanets. Another planet finder named the Transiting Exoplanet Survey Satellite (TESS)[12] will be launched in 2018. It will monitor the brightness of 200000 stars during two years from space, searching for planetary transits. It mainly searches for small planets orbiting bright stars in the solar neighborhood, in order to get detailed observations of the planetary environment and atmosphere. Together with the Next-Generation Transit Survey (NGTS) in Chile, it can discover and tag interesting planets for further research, for example with the JWST. PLATO[13] is a space observatory that will be launched in 2025. Its goal is to find exoplanet systems, especially Earth-sized planets and super-Earths situated in HZ of their host star. Next to that identifying interesting planets for follow-up research on their atmospheres is a goal. Other planned space observatories include WFIRST and CHEOPS. Planned in 2020, WFIRST[14] will use microlensing to find planets in the inner Milky Way and will use coronagraphy to perform high contrast imaging and spectroscopy on individual nearby planets. CHEOPS[15] has its launch planned in 2018 and measure transits around bright stars that are already known to host planets. This way it will target planets for further atmospheric characterization. Ground observatories as SUPERWASP[16] and MASCARA[17] are still searching for exoplanets. The E-ELT[15] will also perform radial velocity searches to discover Earth-like planets from its start in 2024. Next to that it can provide direct imaging of larger planets, possibly including atmospheric characterization. Another candidate for a 2026 ESA mission is ARIEL[18], which will observe exoplanets ranging from Earth- to Jupiter size. It will take spectra and photometric data in order to determine atmospheric compositions. All these new missions will greatly increase the amount of exoplanets discovered as well as the knowledge about them, eventually leading to the confirmation of a habitable planet.

[11] More information about the JWST: https://jwst.nasa.gov/origins.html
[12] More information about TESS: https://tess.gsfc.nasa.gov/overview.html
[13] More information about PLATO: http://sci.esa.int/plato/42277-science/
[14] More information about WFIRST: https://wfirst.gsfc.nasa.gov/exoplanets.html
[15] More information about CHEOPS: http://cheops.unibe.ch/cheops-mission/executive-summary/
[16] More information about SUPERWASP: http://www.superwasp.org/how.htm
[17] More information about MASCARA: http://mascara1.strw.leidenuniv.nl/science/
[18] More information about ELT: http://www.eso.org/public/teles-instr/elt/elt_exo/

References

W.J. Borucki, E. Agol, and F. Fressin et al. Kepler-62: A five-planet system with planets of 1.4 and 1.6 Earthradii in the Habitable Zone. *Science*, 340(6132), 2013.

G.M. Clemence. The Relativity Effect in Planetary Motions. *Rev. Mod. Phys.*, (19):361–364, 1947. 19, 361 – Published 1 October 1947.

F.E. DeMeo and B. Carry. The taxonomic distribution of asteroids from multi-filter all-sky photometric surveys. *Icarus*, 226(1):723–741, sep 2013.

M.S. Dodd, D. Papineau, and T. Grenne et al. Evidence for early life in Earth's oldest hydrothermal vent precipitates. *Nature*, (543):60–64, 2017.

D.A. Fischer, A.W. Howard, and G.P. Laughlin et al. Exoplanet Detection Techniques. *Protostars and Planets*, VI:715–737, may 2015.

M. Gillon, A.H. Triaud, and B.O. Demory et al. Seven temperate terrestrial planets around the nearby ultracool dwarf star TRAPPIST-1. *Nature*, 542(7642):456–460, feb 2017.

M. Griessmeier, A. Stadelmann, and U. Motschmann et al. Cosmic Ray Impact on Extrasolar Earth-Like Planets in Close-in Habitable Zones. *Astrobiology*, 5(5): 587–603, oct 2005. U. MOTSCHMANN.

M. Güdel, N. Erkaev, and J.F. Kasting et al. Astrophysical Conditions for planetary habitability. *Protostars and Planets VI*, University of Arizona Press,:883–906, 2014.

Y. Hu and J. Yang. Role of ocean heat transport in climates of tidally locked exoplanets around M dwarf stars. *PNAS*, 111(2):629–634, jan 2014.

S. Ida and D.N.C. Lin. Toward a deterministic model of planetary formation. I. A desert in the mass and semimajor axis distributions of extrasolar planets. *The Astrophysical Journal*, 604: 388–413, mar 2004.

M. Ikoma and H. Genda. Constraints on the Mass of a Habitable Planet with Water of Nebular Origin. *The Astrophysical Journal*, 648(1):696–706, sep 2006.

B.M. Jakosky, R.P. Lin, and J.M. Grebowsky et al. The Mars Atmosphere and Volatile Evolution (MAVEN) mission. *Space Science Reviews*, 195:3–48, apr 2015.

D. Jontof-Hutter, J.F. Rowe, and J.J. Lissauer et al. The mass of the Mars-sized exoplanet Kepler-138 b from transit timing. *Nature*, 522: 321–323, jun 2015.

L. Kaltenegger and W.A. Traub. Transits of Earth-like planets. *The Astrophysical Journal*, 698(1), may 2009.

D.M. Kass and Y.L. Yung. Loss of atmosphere from Mars due to solar-wind sputtering. *Science*, 268(5211):697–699, may 1995.

J.F. Kasting and D. Catling. Evolution of a Habitable Planet. *Annu. Rev. Astron. Astrophys.*, 4(1), jul 2003.

J.F. Kasting, D.P. Whitmire, and R.T. Reynolds. Habitable Zones around Main Sequence Stars. *Icarus*, 101(1):102–128, jan 1993.

R.K. Kopparapu, R.M. Ramirez, and J. SchottelKotte. Habitable Zones Around Main-Sequence Stars: Dependence on Planetary Mass. *The Astrophysical Journal Letters*, 787 (29), jun .

R.K. Kopparapu, R. Ramirez, and J.F. Kasting et al. Habitable Zones around Main-Sequence stars: new estimates. *The Astrophysical Journal*, 765(2), feb 2013.

R.K. Kopparapu, E.T. Wolf, and J. Haqq-Misra et al. The inner edge of the habitable zone for synchronously rotating planets around low-mass stars using general circulation models. *The Astrophysical Journal*, 819(84), mar 2016.

H. Lammer, J.H. Bredehøft, and A. Coustenis et al. What makes a planet habitable? *Astron. Astrophys. Rev.*, (17):181–249, apr 2009.

W. Ludwig, S. Eggl, and D. Neubauer. Effective stellar flux calculations for limits of life-supporting zones of exoplanets. *Mon.Not.Roy.Astron.Soc.*, 458(4):3752–3759, jun 2016. (2016) 458 (4):.

J.G. Luhmann and T.E Cravens. Magnetic Fields in the ionosphere of Venus. *Space Sci Rev*, 55: 201–274, 1991.

G. Manhes, C.J. Allègre, B. Dupré, and B. Hamelin. Lead isotope study of basic-ultrabasic layered complexes: Speculations about the age of the earth and primitive mantle characteristics. *Earth and Planetary Science letters*, 47(3):370–382, 1980.

C.P. McKay and H.D. Smith. Possibilities for methanogenic life in liquid methane on the surface of Titan. *Icarus*, 178(1):274–276, nov 2005.

H. Mizuno, K. Nakazawa, and C. Hayashi. Instability of a gaseous envelope surrounding a planetary core and formation of giant planets. *Progress of Theoretical Physics*, 60(3):699–710, sep 1978.

A. Morbidelli, J. Chambersz, and J.I. Lunine et al. Source regions and timescales for the delivery of water to the Earth. *Meteoritics and Planetary Science*, (35):1309–1320, 2000.

D. Neubauer, A. Vrtala, and J.J. Leitner et al. Development of a Model to Compute the Extension of Life Supporting Zones for Earth-Like Exoplanets. *Origins of Life and Evolution of Biospheres*, 41(6):545–552, dec 2011.

R.W. Noyes, L.W. Hartmann, and S.L. Baliunas et al. Rotation, convection, and magnetic activity in lower main-sequence stars. *The Astrophysical Journal*, 279:763–777, apr 1984.

D.P. O'Brien, K.J. Walsh, and A. Morbidelli et al. Water Delivery and Giant Impacts in the 'Grand Tack' Scenario. *Icarus*, 239:74–84, sep 2014.

S.J. Paardekooper, C. Baruteau, and W. Kley. A torque formula for non-isothermal Type I planetary migration – II. Effects of diffusion. *Mon.Not.Roy.Astron.Soc.*, 410(1):293–303, jan 2011.

N.R. Pace. The universal nature of biochemistry. *PNAS*, 98(3):805–808, jan 2001.

E. V. Quintana, T. Barclay, and S. N. Raymond et al. An Earth-Sized Planet in the Habitable Zone of a Cool Star. *Science*, 344(6181):277–280, apr 2014.

S.N. Raymond and A. Morbidelli. Making other earths: dynamical simulations of terrestrial planet formation and water delivery. *Icarus*, 168 (1):1–17, mar 2004.

I. Ribas, E. Bolmont, and F. Selsis et al. The habitability of Proxima Centauri b: I. Irradiation, rotation and volatile inventory from formation to the present. *Astronomy & Astrophysics*, 596(111), sep 2016.

T.D. Robinson. Characterizing Exoplanets for Habitability. *Handbook for exoplanets*, jan 2017.

D. Schulze-Makuch and L.N. Irwin. The prospect of alien life in exotic forms on other worlds. *Naturwissenschaften*, 93(4):155–172, apr 2006.

S. Seager. *Exoplanets*. University of Arizona Press, 2010.

S. Seager. Exoplanet Habitability. *Science*, 340 (6132):577–581, may 2013.

S. Seager and D. Deming. Exoplanet Atmospheres. *Annu. Rev. Astron. Astrophys.*, 48: 631–672, jun 2010.

S. Seager, M. Kuchner, A. Hier-Majumder, and Militzer B. Mass-Radius Relationships for Solid Exoplanets. *The Astrophysical Journal*, 669(2): 1279–1297, nov 2007.

F. Selsis, J.F. Kasting, and B. Levrard et al. Habitable planets around the star Gliese 581? *Astronomy & Astrophysics*, 476:1373–1387, oct 2007.

D.S. Spiegel, S.N. Raymond, and C.D. Dressing et al. Generalized Milankovitch Cycles and Long-Term Climatic Habitability. *The Astrophysical Journal*, 721(2):1308–1318, oct 2010.

M.R. Swain, G. Tinetti, and G. Vasish et al. Water, Methane and Carbon Dioxide present in the dayside spectrum of the exoplanet HD 209458b. *The Astrophysical Journal*, 704(2), 2009.

M. Turbet, M. Leconte, and F. Selsis et al. The habitability of Proxima Centauri b: II. Possible climates and observability. *Astronomy & Astrophysics*, 596(A112), sep 2016.

G. Vladilo, G. Murante, and L. Silva et al. The habitable zone of Earth-like planets with different levels of atmospheric pressure. *The Astrophysical Journal*, 767(1), mar 2013.

S.S. Vogt, J. Burt, and S. Meschiari et al. Six planets orbiting HD 219134. *The Astrophysical Journal*, 814(12), 2015.

L.M. Weiss and G.W. Marcy. The mass-radius relation for 65 exoplanets smaller than 4 Earth radii. *The Astrophysical Journal Letters*, 783 (L6), mar 2014.

J. Yang, N. Cowan, and D. Abbot. Stabilizing cloud feedback dramatically expands the habitable zone of tidally locked planets. *The Astrophysical Journal*, 771(2), jun 2013.

A Appendix: Python code

```
from __future__ import print_function, division
import matplotlib.pyplot as plt
import numpy as np
import pylab
import matplotlib.pyplot as plt
import matplotlib.patches as patches
import math
%matplotlib inline

#opening data
#file only containing the discovery method and the associated discovery year
method, yeardis = np.genfromtxt('planets.csv', delimiter=",", usecols=(1,3), unpack=
    True)
#file containing data only about planet TRAPPIST 1c
trapp=np.genfromtxt ('trappist1c.csv', delimiter=",", unpack=True)
#file containing necessary data about all exoplanets
data=np.genfromtxt ('parameters.csv', delimiter=",", unpack=True)
rowid=data[0] #row numbers for planets
###plot of the amount of planets found per year
method1=[]
method2=[]
method3=[]
method4=[]
method5=[]
#including used detection methods
for i in range(len(method)):
    if method[i]==1:
        method1.append(yeardis[i])
    elif method[i]==2:
        method2.append(yeardis[i])
    elif method[i]==3:
        method3.append(yeardis[i])
    elif method[i]==4:
        method4.append(yeardis[i])
    elif method[i]==5:
        method5.append(yeardis[i])

#plotting into cumulative histogram
pylab.figure(figsize=(10,10))
pylab.ylabel('Number of exoplanets')
pylab.xlabel('Year')
pylab.xlim(1989, 2017)
bins_all=29
hist= pylab.hist([method1,method2,method3,method4,method5],label=['Radial Velocity', '
    Transit',
                                'Imaging', 'Microlensing', 'Other'], bins=bins_all,
                                histtype='bar', stacked=True, cumulative=True)
pylab.legend(loc='best')
pylab.show()

####Equilibrium Temperature: TRAPPIST 1C
#getting data for TRAPPIST 1C
sigma=5.67*10**-8 #W m^-2 K^-1
lumlog=trapp[56] #luminosity in log(lum_sun)
lumlog=lumlog[~np.isnan(lumlog)] #not using NaN values
lumlogmax=lumlog+0.027 #upper limit
lumlogmin=lumlog-0.029 #lower limit
stellum=(10**lumlog)*3.848*10**26  #logscale to watts
stellummax=(10**lumlogmax)*3.848*10**26  #including uncertainties
stellummin=(10**lumlogmin)*3.848*10**26
semmajtr=(trapp[8])  #distance to host star in AU
semmajtr=semmajtr[~np.isnan(semmajtr)]
semmajmax=semmajtr+0.00000170  #upper limit
semmajmin=semmajtr-0.00000170  #lower limit
distance=semmajtr*149597870700  #AU to m
distancemax=semmajmax*149597870700  #including uncertainties
distancemin=semmajmin*149597870700
```

```
#upper and lower limit of equil temperature
uppert=((stellummax*(1-0.95))/(4*np.pi*(distancemax**2)*2*sigma))**(1/4)
lowert=((stellummin*(1-0.95))/(4*np.pi*(distancemin**2)*2*sigma))**(1/4)


#defining the different albedo values used
A=[0, 0.068, 0.11, 0.25, 0.306, 0.4, 0.5
    , 0.6, 0.7, 0.77, 0.9, 0.95, 0.98, 0.995, 1.0]

#calculation of equilibrium temperature
def T_eq(A):    #redistribution factor f=4
    return ((stellum*(1-A))/(4*np.pi*(distance**2)*4*sigma))**(1/4)

def T_eq2(A):   #redistribution factor f=2
    return ((stellum*(1-A))/(4*np.pi*(distance**2)*2*sigma))**(1/4)

#creating lists with the eq temps
Teq=[]
Teq2=[]
for albedo in A:
    T=T_eq(albedo)
    Teq.append(T)
    T2=T_eq2(albedo)
    Teq2.append(T2)

#get the associated uncertainty percentages, values to be adjusted
print('Uncertainties in Teq:', (Teq2[11]-uppert)/Teq2[11], (Teq2[11]-lowert)/Teq2[11])


#plotting of TRAPPIST 1c eq temps while including ranges maybe capable of life support
fig, ax = plt.subplots(figsize=(10, 10))
plt.plot(Teq, A, linestyle='-', marker='o', color='blue', label='f=4')
plt.plot(Teq2, A, linestyle='-', marker='o', label='f=2', color='red')
plt.axhline(y=0.77, ls='--', color='black', label='Bond albedo of Venus')
plt.axhline(y=0.068, color='black', label='Bond albedo of Mercury')
ax.add_patch(patches.Rectangle((273.15, 0),100,1, alpha=0.2, color='green', label='
    Liquid water Range'))
ax.add_patch(patches.Rectangle((90.69, 0),20.98,1, alpha=0.2, color='blue', label='
    Liquid methane Range'))
ax.add_patch(patches.Rectangle((195.41, 0),44.41,1, alpha=0.2, color='red', label='
    Liquid ammonia Range'))
ax.add_patch(patches.Rectangle((63.15, 0),14.2,1, alpha=0.2, color='orange', label='
    Liquid nitrogen Range'))
plt.legend(loc='best', scatterpoints=1, numpoints=1, fontsize=12)
plt.xlabel('Equilibrium Temperature [K]', fontsize=14)
plt.ylabel('Bond Albedo', fontsize=14)
plt.show()

###Equilibrium Temperature: other exoplanets
sigma=5.67*10**-8 #W m^-2 K^-1
lumlogall=data[41]
#luminosity=lumlogall[~np.isnan(lumlogall)]
stellumall=(10**lumlogall)*3.848*10**26  #logscale to watts
semmajall=(data[8])
#semmajall=semmajall[~np.isnan(semmajall)]
distanceall=(semmajall*149597870700)**2 #AU to m/already squared for equilibrium temp

#creating lists for the exoplanets that have both distance to host star as well as
    luminosity known
distanceall2=[]
stellumall2=[]
for i in range(len(distanceall)):
    for j in range(len(stellumall)):
        if i==j:
            distanceall2.append(distanceall[i])
            stellumall2.append(stellumall[j])
x=np.array(distanceall2)
y=np.array(stellumall2)
```

```
#calculation of eq temps
def T_eq(A):    #redistribution factor f=4
    return ((y*(1-A))/(4*np.pi*(x*4*sigma)))**(1/4)

def T_eq2(A):   #redistribution factor f=2
    return ((y*(1-A))/(4*np.pi*(x*2*sigma))**(1/4))

#lists for the eq temps
Teqall=[]   #f=4
Teqall2=[]  #f=2
for albedo in A:
    teq=T_eq(albedo)
    Teqall.append(teq)
    teq2=T_eq2(albedo)
    Teqall2.append(teq2)

#plotting of the eq temps for different albedo values
#albedo 0.068, 0.306 and 0.77 separately plotted
#different liquid ranges also again indicated in plots
z=np.sqrt(x)/149597870700  #using x-axis as distance in AU
fig= plt.figure(figsize=(15,15))
fig.text(0.5, 0.09, 'Orbit Semi-Major Axis [AU]', fontsize=14, ha='center')
fig.text(0.07, 0.5, 'Equilbrium Temperature [K]', fontsize=14, va='center', rotation='
    vertical')
ax1=fig.add_subplot(221)
ax1.plot(z, Teqall[0], 'o', color='turquoise', label='Albedo=0')
ax1.plot(z, Teqall[1], 'o', color='red', label='Albedo=0.068')
ax1.plot(z, Teqall[2], 'o', color='blue', label='Albedo=0.11')
ax1.plot(z, Teqall[3], 'o', color='violet', label='Albedo=0.25')
ax1.plot(z, Teqall[4], 'o', color='green', label='Albedo=0.306')
ax1.plot(z, Teqall[5], 'o', color='cyan', label='Albedo=0.4')
ax1.plot(z, Teqall[6], 'o', color='magenta', label='Albedo=0.5')
ax1.plot(z, Teqall[7], 'o', color='yellow', label='Albedo=0.6')
ax1.plot(z, Teqall[8], 'o', color='grey', label='Albedo=0.7')
ax1.plot(z, Teqall[9], 'o', color='black', label='Albedo=0.77')
ax1.plot(z, Teqall[10], 'o', color='white', label='Albedo=0.9')
ax1.plot(z, Teqall[11], 'o', color='orange', label='Albedo=0.95')
ax1.plot(z, Teqall[12], 'o', color='pink', label='Albedo=0.98')
ax1.plot(z, Teqall[13], 'o', color='navy', label='Albedo=0.995')
ax1.add_patch(patches.Rectangle((0, 90.7),6, 20.96, alpha=0.2, color='blue'))
ax1.add_patch(patches.Rectangle((0, 195.41),6, 44.41, alpha=0.2, color='red'))
ax1.add_patch(patches.Rectangle((0, 273.15),6, 100, alpha=0.2, color='green'))
ax1.add_patch(patches.Rectangle((0, 63.15),6, 14.2, alpha=0.2, color='orangered'))
ax1.set_xlim(0,6)
ax1.set_ylim(0,1000)
ax1.legend(loc='best', numpoints=1)
ax2=fig.add_subplot(222)
ax2.plot(z, Teqall[1], 'o')
ax2.add_patch(patches.Rectangle((0, 90.69),6, 20.98, alpha=0.2, color='blue', label='
    Liquid methane Range'))
ax2.add_patch(patches.Rectangle((0, 195.41),6, 44.41, alpha=0.2, color='red', label='
    Liquid ammonia Range'))
ax2.add_patch(patches.Rectangle((0, 273.15),6, 99.97, alpha=0.2, color='green',  label='
    Liquid water Range'))
ax2.add_patch(patches.Rectangle((0, 63.15),6, 14.2, alpha=0.2, color='orangered', label=
    'Liquid nitrogen Range'))
ax2.legend(title='Bond albedo=0.068', loc='best')
ax2.set_xlim(0,6)
ax2.set_ylim(0,1000)
ax3 = fig.add_subplot(223)
ax3.plot(z, Teqall[4], 'o')
ax3.add_patch(patches.Rectangle((0, 90.69),6, 20.98, alpha=0.2, color='blue', label='
    Liquid methane Range'))
ax3.add_patch(patches.Rectangle((0, 195.41),6, 44.41, alpha=0.2, color='red', label='
    Liquid ammonia Range'))
ax3.add_patch(patches.Rectangle((0, 273.15),6, 99.97, alpha=0.2, color='green', label='
    Liquid water Range'))
ax3.add_patch(patches.Rectangle((0, 63.15),6, 14.2, alpha=0.2, color='orangered', label=
    'Liquid nitrogen Range'))
ax3.set_xlim(0,6)
```

```
ax3.set_ylim(0,1000)
ax3.legend(title='Bond albedo=0.306', loc='best')
ax4=fig.add_subplot(224)
ax4.plot(z, Teqall[9], 'o')
ax4.add_patch(patches.Rectangle((0, 90.69),6, 20.98, alpha=0.2, color='blue', label='
    Liquid methane Range'))
ax4.add_patch(patches.Rectangle((0, 195.41),6, 44.41, alpha=0.2, color='red', label='
    Liquid ammonia Range'))
ax4.add_patch(patches.Rectangle((0, 273.15),6, 99.97, alpha=0.2, color='green', label='
    Liquid water Range'))
ax4.add_patch(patches.Rectangle((0, 63.15),6, 14.2, alpha=0.2, color='orangered', label=
    'Liquid nitrogen Range'))
ax4.set_xlim(0,6)
ax4.set_ylim(0,1000)
ax4.legend(title='Bond albedo=0.77', loc='best')
fig.show()

#creating list for number of exoplanets in different
#liquid ranges
waterrange=[]
methanerange=[]
ammoniarange=[]
nitrogenrange=[]
for i in Teqall[4]:
    if 273.15<=i<=373.12:
        waterrange.append(i)
    elif 90.69<=i<=111.67:
        methanerange.append(i)
    elif 195.41<=i<=239.82:
        ammoniarange.append(i)
    elif 63.15<=i<=77.35:
        nitrogenrange.append(i)
#getting number of exoplanets per range
print('number of planets for water, methane, ammonia, nitrogen')
print(len(waterrange), len(methanerange), len(ammoniarange), len(nitrogenrange))

###Calculation of HZ: TRAPPIST 1c
#Tmax is boiling point different solvents
Tmax=[373.12, 111.67, 239.82, 77.35] #K
#Tmin is freezing point different solvents
Tmin=[273.15, 90.69, 195.41, 63.15] #K

#first for f=2, only using water
def mind(A):  #inner limit HZ with boiling point of water
    return ((stellum*(1-A))/(4*np.pi*sigma*2*373.12**4))**(1/2)/149597870700
def maxd(A):  #outer limit HZ with freezing point of water
    return ((stellum*(1-A))/(4*np.pi*sigma*2*273.15**4))**(1/2)/149597870700
#f=4
def mind2(A):
    return ((stellum*(1-A))/(4*np.pi*sigma*4*373.12**4))**(1/2)/149597870700
def maxd2(A):
    return ((stellum*(1-A))/(4*np.pi*sigma*4*273.15**4))**(1/2)/149597870700

#creating lists to store the HZ boundaries
maxdist=[] #f=2
mindist=[]
maxdist2=[] #f=4
mindist2=[]
for albedo in A:
    d=maxd(albedo)
    maxdist.append(d)
    d2=mind(albedo)
    mindist.append(d2)
    df=maxd2(albedo)
    maxdist2.append(df)
    df2=mind2(albedo)
    mindist2.append(df2)


#plotting the Bond Albedo vs HZ boundaries, for different f values
```

```
fig, ax = plt.subplots(figsize=(10, 10))
plt.plot(maxdist, A, linestyle='-', marker= 'o', label='f=2, outer', color='blue')
plt.plot(mindist, A, linestyle='-', marker= 'o', label='f=2, inner', color='red')
plt.plot(maxdist2, A, linestyle='-', marker= 'o', label='f=4, outer', color='green')
plt.plot(mindist2, A, linestyle='-', marker= 'o', label='f=4, inner', color='grey')
plt.legend(loc='best', scatterpoints=1, numpoints=1, fontsize=12)
plt.xlabel('Distance from host star [AU]', fontsize=14)
plt.ylabel('Bond Albedo', fontsize=14)
plt.show()

#print outer and inner boundaries HZ, for common albedos
print('The HZ boundaries for TRAPPIST 1 are:')
print(mind(0.068), maxd(0.068), 'f=2 for Mercury albedo')
print(mind2(0.068), maxd2(0.068), 'f=4 for Mercury albedo')
print(mind(0.306), maxd(0.306), 'f=2 for Earth albedo')
print(mind2(0.306), maxd2(0.306), 'f=4 for Earth albedo')
print(mind(0.77), maxd(0.77), 'f=2 for Venus albedo')
print(mind2(0.77), maxd2(0.77), 'f=4 for Venus albedo')

#get the associated uncertainties, values to be adjusted
upperdismin=((stellummax*(1-0.068))/(4*np.pi*sigma*2*273.15**4))**(1/2)/149597870700
lowerdismin=((stellummin*(1-0.068))/(4*np.pi*sigma*2*273.15**4))**(1/2)/149597870700
percent1=maxd(0.068)-lowerdismin
percent2=maxd(0.068)-upperdismin
print('Uncertainties in Trappist-1 HZ:', percent1/maxd(0.068), percent2/maxd(0.068))

###Influence of CO2 on HZ boundaries: TRAPPIST 1C
Teff2=trapp[24]   #effective stellar temperature
Teff=Teff2[~np.isnan(Teff2)]  #removing NaN values
Tstar=Teff-5780  #star temp for effective flux
stellumsol=(10**lumlog)   #star luminosity / solar luminosity

# 1 bar and 8 bar CO2 atmosphere respectively
seffco2=[0.6774, 0.4594]
aco2=[3.3998*10**-5, 6.7254**-5]
bco2=[1.0272*10**-8, 3.3246*10**-9]
#stellar effective flux
seffonebar=seffco2[0]+aco2[0]*Tstar+bco2[0]*Tstar**2
seffeightbar=seffco2[1]+aco2[1]*Tstar+bco2[1]*Tstar**2
#outer limits in AU for CO2: max greenhouse
outeronebar=(stellumsol/seffonebar)**0.5
outereightbar=(stellumsol/seffeightbar)**0.5
print('The HZ for:')
print('1bar CO2:', outeronebar, '8bar CO2:', outereightbar)

###HZ boundaries via greenhouse effects
#runaway greenhouse, moist greenhouse, maximum greenhouse factors
a=[1.3242*10**(-4), 8.1774*10**(-5), 5.8942*10**(-5)]
b=[1.5418*10**(-8), 1.7063*10**(-9), 1.6558*10**(-9)]
c=[-7.9895*10**(-12), -4.3241*10**(-12), -3.0045*10**(-12)]
d=[-1.8328*10**(-15), -6.6462*10**(-16), -5.2983*10**(-16)]
#effective solar flux for different greenhouses
ssolar=[1.0512, 1.0140, 0.3438]
#Calculation of HZ boundaries for the factors
#effective stellar flux
Seffrun=ssolar[0]+a[0]*Tstar+b[0]*Tstar**2+c[0]*Tstar**3+d[0]*Tstar**4
Seffmoist=ssolar[1]+a[1]*Tstar+b[1]*Tstar**2+c[1]*Tstar**3+d[1]*Tstar**4
Seffmax=ssolar[2]+a[2]*Tstar+b[2]*Tstar**2+c[2]*Tstar**3+d[2]*Tstar**4
#HZ distance in AU
innerrun=(stellumsol/Seffrun)**0.5
innermoist=(stellumsol/Seffmoist)**0.5
outermax=(stellumsol/Seffmax)**0.5
print('Inner runaway:', innerrun, 'Inner moist:', innermoist, 'outer max:', outermax)

###eccentricities
#opening necessary data
eccen= data[12]
semmaj=data[8]

eccent=eccen[~np.isnan(eccen)]  #removing NaN's
```

```
#creating lists for eccentricities with sem maj axis
eccen1=[]
eccen2=[]
eccen3=[]
eccen4=[]
eccen5=[]
#including associated semi major axis
for i in range(len(eccent)):
    if semmaj[i] <=1:
        eccen1.append(eccen[i])
    elif 1< semmaj[i]<=2:
        eccen2.append(eccen[i])
    elif 2< semmaj[i]<=3:
        method3.append(eccen[i])
    elif 3< semmaj[i]<=4:
        eccen4.append(eccen[i])
    elif semmaj[i]>=4:
        eccen5.append(eccen[i])

#histogram with the different eccentricity values for all exoplanets
pylab.figure(figsize=(10,10))
pylab.ylabel('Number of exoplanets', fontsize=14)
pylab.xlabel('Eccentricity', fontsize=14)
hist= pylab.hist(eccent, bins=58, stacked=True, histtype='bar')
pylab.axvline(x=0.205, color='violet', linestyle='dashed', linewidth=2, label='Mercury')
pylab.axvline(x=0.007, color='r', linestyle='dashed', linewidth=2, label='Venus')
pylab.axvline(x=0.017, color='g', linestyle='dashed', linewidth=2, label='Earth')
pylab.axvline(x=0.094, color='y', linestyle='dashed', linewidth=2, label='Mars')
pylab.legend(loc='best', fontsize=12)
pylab.show()
#including the semi major axis of the planets
pylab.figure(figsize=(10,10))
pylab.ylabel('Number of exoplanets', fontsize=14)
pylab.xlabel('Eccentricity', fontsize=14)
pylab.ylim(0,36)
hist= pylab.hist([eccen1,eccen2,eccen3,eccen4,eccen5],label=['$\leq1$', '$1<$semmaj$\
    leq2$',
                                '$2<$semmaj$<\leq3$', '$3<$semmaj$\leq4$', '>4'], bins
    =58, stacked=True, histtype='bar')
pylab.legend(title='Semi-Major axis values in AU', loc='best', fontsize=12)
pylab.show()


###Maximum eccentricities
def maxeccent(a,b):    #a=semi major axis, b=semi minor axis
    return (1-b**2/a**2)**(1/2)

#use boiling and freezing points as boundaries of HZ
#and hence as semi major and semi minor axis
Tmax=[373.12, 111.67, 239.82, 77.35] #water, methane, ammonia, nitrogen
Tmin=[273.15, 90.69, 195.41, 63.15]
def mindsol(T): #gives semi minor axis
    return ((stellum*(1-0.306))/(4*np.pi*sigma*2*T**4))**(1/2)/149597870700
def maxdsol(T): #gives semi major axis
    return ((stellum*(1-0.306))/(4*np.pi*sigma*2*T**4))**(1/2)/149597870700

#calculate the maximum eccentricity for the different solvents
print('The maximum eccentricities for water, methane, ammonia, nitrogen are:')
for i in range(len(Tmax)):
    for j in range(len(Tmin)):
        if i==j:
            b=mindsol(Tmax[i])
            a=maxdsol(Tmin[j])
            print(maxeccent(a,b))

#plot of eccentricity vs sem maj axis with max
#eccentricities included, not very helpfull
fig, ax = plt.subplots(figsize=(10,10))
plt.plot(semmaj, eccen, 'o', ls='none', color='green', label='Exoplanet')
```

```
plt.axhline(y=0.844264, color='blue', label='Max eccentricity water')
plt.axhline(y=0.751663, color='cyan', label='Max eccentricity methane')
plt.axhline(y=0.747794, color='black', label='Max eccentricity ammonia')
plt.axhline(y=0.745470, color='orange', label='Max eccentricity nitrogen')
plt.xlim(0,5)
plt.ylim(0,1)
plt.legend(loc='best', scatterpoints=1, numpoints=1)
plt.xlabel('Orbit Semi-Major Axis[AU]', fontsize=14)
plt.ylabel('Eccentricity', fontsize=14)
plt.show()
print('total eccentricities known:', len(eccent))

#creating lists for planets that apply to the eccentricity ranges
watereccent=[]
othereccent=[]
for i in eccent:
    if i<0.844264:
        watereccent.append(i)
for i in eccen:
    if i<0.751663:
        othereccent.append(i)
#print number of planets in appropriate eccentricity ranges
print('number of planets with the appropriate eccentricity:')
print('for water as solvent:', len(watereccent), ' and other solvents:', len(othereccent
    ))

###Plots of mass, radius, density
#getting necessary data
orbmax=data[8]
mass = data[33]
radius = data[37]
density = data[16]
densupper= data[17]
denslower= data [18]

#plotting mass vs density and radius vs density
#to show that the mass limit works
fig, ax = plt.subplots(figsize=(10, 10))
plt.plot(mass,density,'o')
plt.errorbar(mass, density, yerr=(-densupper, denslower), fmt='o', ls='none', color='
    green', label='Exoplanet')
plt.plot(1, 5.514, marker='^', markersize=7, color="blue", label='Earth', linestyle = '
    None')
plt.plot(0.107, 3.933, marker='^', markersize=7, color="red", label='Mars', linestyle =
    'None')
plt.plot(0.815, 5.243, marker='^', markersize=7, color="orange", label='Venus',
    linestyle = 'None')
#plt.plot(317.83, 1.326, marker='^', markersize=7, color="cyan", label='Jupiter',
    linestyle = 'None')
plt.plot(17.15, 1.638, marker='^', markersize=7, color="magenta", label='Neptune',
    linestyle = 'None')
#plt.plot(95.16, 0.687, marker='^', markersize=7, color="black", label='Saturn',
    linestyle = 'None')
plt.plot(0.0553, 5.427, marker='^', markersize=7, color="grey", label='Mercury',
    linestyle = 'None')
plt.plot(14.54, 1.271, marker='^', markersize=7, color="violet", label='Uranus',
    linestyle = 'None')
plt.xlim(0, 40)
plt.ylim(0,20)
plt.xlabel('Planet mass [$ M_{\oplus}$]', fontsize=14)
plt.ylabel('Planet density [$g/cm^3$]', fontsize=14)
plt.legend(loc='best', scatterpoints=1, numpoints=1, fontsize=12)
plt.show()

#plotting radius vs density to show that the  radius limit works
fig, ax = plt.subplots(figsize=(10, 10))
ax.errorbar(radius, density, yerr=(-densupper, denslower), fmt='o', ls='none', color='
    green', label='Exoplanet')
plt.plot(1, 5.514, marker='^', markersize=7, color="blue", label='Earth', linestyle = '
    None')
```

```
plt.plot(0.532, 3.933, marker='^', markersize=7, color="red", label='Mars', linestyle = 'None')
plt.plot(0.949, 5.243, marker='^', markersize=7, color="orange", label='Venus', linestyle = 'None')
plt.plot(11.209, 1.326, marker='^', markersize=7, color="cyan", label='Jupiter', linestyle = 'None')
plt.plot(3.883, 1.638, marker='^', markersize=7, color="magenta", label='Neptune', linestyle = 'None')
plt.plot(9.449, 0.687, marker='^', markersize=7, color="black", label='Saturn', linestyle = 'None')
plt.plot(0.383, 5.427, marker='^', markersize=7, color="grey", label='Mercury', linestyle = 'None')
plt.plot(4.007, 1.271, marker='^', markersize=7, color="violet", label='Uranus', linestyle = 'None')
plt.xlim(0, 20)
plt.ylim(0,20)
plt.xlabel('Planet radius [$ R_{\oplus}$]', fontsize=14)
plt.ylabel('Planet density [$g/cm^3$]', fontsize=14)
plt.legend(loc='best', scatterpoints=1, numpoints=1, fontsize=12)
plt.show()


#plotting mass vs radius
fig, ax = plt.subplots(figsize=(10, 10))
plt.scatter(mass, radius, label='Exoplanets')
plt.xlabel('Planet mass [$ M_{\oplus}$]', fontsize=14)
plt.ylabel('Planet radius [$ R_{\oplus}$]', fontsize=14)
plt.xscale('log')
plt.xlim(0.01,10000)
plt.ylim(0,25)
ax.add_patch(patches.Rectangle((0, 0),10,2, alpha=0.2))    #rocky surface ranges
plt.plot(1, 1, marker='^', markersize=7, color="green", label='Earth', linestyle = 'None')
plt.plot(0.107, 0.532, marker='^', markersize=7, color="red", label='Mars', linestyle = 'None')
plt.plot(0.815, 0.949, marker='^', markersize=7, color="orange", label='Venus', linestyle = 'None')
plt.plot(317.83, 11.209, marker='^', markersize=7, color="cyan", label='Jupiter', linestyle = 'None')
plt.plot(17.15, 3.883, marker='^', markersize=7, color="magenta", label='Neptune', linestyle = 'None')
plt.plot(95.16, 9.449, marker='^', markersize=7, color="black", label='Saturn', linestyle = 'None')
plt.plot(0.0553, 0.383, marker='^', markersize=7, color="grey", label='Mercury', linestyle = 'None')
plt.plot(14.54, 4.007, marker='^', markersize=7, color="violet", label='Uranus', linestyle = 'None')
plt.legend(loc='upper left', scatterpoints=1, numpoints=1, fontsize=12)
plt.show()


mass1=[]   #inserting mass range for rocky planets
row1=[]
row2=[]
for i in range(len(mass)):
    if mass[i]<10:
        mass1.append(mass[i])
        row1.append(rowid[i])
radius1=[]     #inserting radius range for rocky planets
for j in range(len(radius)):
        if radius[j]<2:
            radius1.append(radius[j])
            row2.append(rowid[j])

#create lists to store planets that follow both criteria
mass2=[]
radius2=[]
for i in row1:     #keeping planets that have both criteria
    for j in row2:
        if i==j:
```

```
            mass2.append(mass[i])
            radius2.append(radius[j])

#plotting the planets that indeed follow the right criteria
fig, ax = plt.subplots(figsize=(10, 10))
plt.scatter(mass2, radius2, label='Exoplanets')
plt.xlabel('Planet mass [$ M_{\oplus}$]', fontsize=14)
plt.ylabel('Planet radius [$ R_{\oplus}$]', fontsize=14)
plt.xlim(0,10)
plt.plot(1, 1, marker='^', markersize=7, color="green", label='Earth', linestyle = 'None')
plt.plot(0.107, 0.532, marker='^', markersize=7, color="red", label='Mars', linestyle = 'None')
plt.plot(0.815, 0.949, marker='^', markersize=7, color="orange", label='Venus', linestyle = 'None')
plt.plot(0.0553, 0.383, marker='^', markersize=7, color="grey", label='Mercury', linestyle = 'None')
plt.legend(loc='best', scatterpoints=1, numpoints=1, fontsize=12)
plt.show()

#Finding the numbers of planets that have both an equilibrium temperature and mass and radius defined
tempnumber=Teqall[0][~np.isnan(Teqall[0])]
massnumber=mass[~np.isnan(mass)]
leftovers=[]
for i in range(len(tempnumber)):
    for j in range(len(massnumber)):
            if i==j:
                leftovers.append(i)


#Finding the habitable planets in the different liquid ranges
row3=[]   #planet id's for water range
row4=[]   #planet id's for methane range
row5=[]   #planet id's for ammonia range
row6=[]   #planet id's for nitrogen range

#Equilibrium temperature, can be adjusted for different
#values of albedo: Teqall[1] for albedo=0.068 etc.
T=Teqall[10]
for i in range(len(T)):
    if 273.15<=T[i]<=373.12:
        waterrange.append(T[i])
        row3.append(rowid[i])
    elif 90.69<=T[i]<=111.67:
        methanerange.append(T[i])
        row4.append(rowid[i])
    elif 195.41<=T[i]<=239.82:
        ammoniarange.append(T[i])
        row5.append(rowid[i])
    elif 63.15<=T[i]<=77.35:
        nitrogenrange.append(T[i])
        row6.append(rowid[i])
#last check is whether the planet also has appropriate
#mass and radius

planetid=[]
planettemp=[]
for i in row1:
    for j in row2:
        for k in row3:
                if i==j==k:
                    planetid.append(rowid[i])
                    planettemp.append(T[i])
print('The habitable planet IDs for this temp range are:', planetid)

###Calculation of HZ's for habitable planets
sigma=5.67*10**-8 #W m^-2 K^-1
stellumhd=(10**-0.5774)*3.848*10**26    #luminosity HD 219134
stellumhdmax=(10**(-0.5774+0.0081))*3.848*10**26 #uncertainties
```

```
stellumhdmin=(10**(-0.5774-0.0083))*3.848*10**26
stellumlhs=(10**-2.526)*3.848*10**26   #luminosity LHS 1140
stellumlhsmax=(10**(-2.526+0.030))*3.848*10**26  #uncertainties
stellumlhsmin=(10**(-2.526-0.032))*3.848*10**26
stellumkep=(10**-0.678)*3.848*10**26   #luminosity Kepler-62
stellumkepmax=(10**(-0.678+0.040))*3.848*10**26  #uncertainties
stellumkepmin=(10**(-0.678-0.043))*3.848*10**26

lumlog=trapp[56] #luminosity TRAPPIST-1
lumlog=lumlog[~np.isnan(lumlog)]
stellum=(10**lumlog)*3.848*10**26  #logscale to watts
#Tmax is boiling point different solvents, hence for inner HZ
Tmax=[373.12, 111.67, 239.82, 77.35] #K
#Tmin is freezing point different solvents, hence for outer HZ
Tmin=[273.15, 90.69, 195.41, 63.15] #K

#luminosity can be adjusted for specific star/planet
def innsol(A): #calculation of inner HZ as function of albedo A
    return ((stellumkep*(1-A))/(4*np.pi*sigma*4*Tmax[1]**4))**(1/2)/149597870700
def outsol(A): #calculation of outner HZ as function of albedo A
    return ((stellumkep*(1-A))/(4*np.pi*sigma*4*Tmin[1]**4))**(1/2)/149597870700

#printing inner and outer limits HZ
print('The HZ limits for the specific solvent and planet are:')
print(innsol(0.068), outsol(0.068))
print(innsol(0.306), outsol(0.306))
print(innsol(0.77), outsol(0.77))
print(innsol(0.9), outsol(0.9))

#calculation of uncertainties, values can be adjusted
#Tmax and innsol needed for inner HZ, Tmin and outsol for outer HZ
#albedo values A can be adjusted, must be done in all 4 formulas
upperdismin1=((stellumkepmax*(1-0.306))/(4*np.pi*sigma*4*Tmax[1]**4))**(1/2)
    /149597870700
lowerdismin1=((stellumkepmin*(1-0.306))/(4*np.pi*sigma*4*Tmax[1]**4))**(1/2)
    /149597870700
percent3=innsol(0.306)-lowerdismin1
percent4=innsol(0.306)-upperdismin1
print('Uncertainty:',percent3/innsol(0.306), percent4/innsol(0.306))
```